


Cite this: *Sustainable Energy Fuels*,  
2025, 9, 3550

# Advancing industrial rate current density in water electrolysis for green hydrogen production: catalyst development, benchmarking, and best practices

Samruddhi V. Chauhan, Kinjal K. Joshi, Pratik M. Pataniya and C. K. Sumesh \*

Green hydrogen production through water electrolysis has emerged as an outstanding and compatible source of sustainable energy. The zero-carbon emission with high purity marks its footprint towards industrialization. However, achieving commercial-scale current density with utmost durability has been a challenge for the research community. Several technical obstacles need to be overcome before its full promise can be realized as a potential alternative to fossil fuels. This review explores the advantages and limitations of non-noble electrocatalysts, highlighting promising strategies such as 3D substrate integration and binder-free synthesis, which enhance water electrolysis and electrochemical performance for industrial hydrogen generation. Promising approaches to effective water dissociation using 3D substrate material are outlined in the work, along with the advantages of binder-free synthesis and sophisticated manufacturing processes that could simplify electrode design while lowering costs and improving performance. This review offers an essential viewpoint on the engineering of green hydrogen in the future by combining these methods. The creation of next-generation water electrolysis systems ensures a sustainable and profitable hydrogen economy while also directly advancing the Sustainable Development Goals (SDGs) of the UN, which include clean energy, industrial innovation, and climate action.

Received 18th February 2025  
Accepted 21st May 2025

DOI: 10.1039/d5se00262a

rsc.li/sustainable-energy

## 1 Introduction

The over-reliance on hydrocarbons has disrupted the environmental balance of our ecosystem. The relentless consumption of fossil fuels has led to increased carbon emissions, posing a significant threat to all forms of life.<sup>1,2</sup> In response, the scientific community is actively exploring alternative renewable energy sources that can support future advancements while prioritizing the safety of our planet and maintaining efficiency.<sup>3</sup>

Hydrogen energy production acts as a boon for mankind by reducing the emissions of hydrocarbons generated by fossil fuels.<sup>4</sup> Hydrogen is a renewable energy source that maintains a balance between economic and environmentally friendly strategies. The dissociation of water molecules into hydrogen and oxygen is facilitated by two half-cell electrochemical reactions: the hydrogen evolution reaction (HER) and the oxygen evolution reaction (OER).<sup>5,6</sup> The primary focus area revolves around the performance of an electrocatalyst that can be anchored to the electrochemical cell. To date, noble metal-based electrocatalysts have played a crucial role in the liberation of H<sub>2</sub>. However, the increasing scarcity and high cost have

heightened the urgency to study catalysts that can compete with the growing demand.

Numerous non-noble electrocatalysts, including transition metal-based electrodes, have been reported in recent decades. These electrodes can exhibit low potential and longer durability at milliampere scale current densities ranging from 10 to 100 mA cm<sup>-2</sup>.<sup>5</sup> However, the criteria for the commercialization of these electrode materials include larger current densities, exceeding 1000 mA cm<sup>-2</sup>, as well as longer and corrosion-free durability.<sup>7</sup> Therefore, the research focus has shifted toward producing electrocatalysts capable of sustaining higher current densities.<sup>8</sup> Nonetheless, increased current density also presents significant technological challenges, including higher energy requirements, issues with heat control, and potential degradation of electrolyzer materials. Consequently, developing advanced materials and technologies is imperative to endure these high current densities and the associated challenges.<sup>9</sup>

In the following review, we have abridged the current progress made for the upliftment of the current density and our views on the development of electrocatalysts that can outperform large scale in harsh conditions. We have elaborated on different non-noble electrocatalysts delivering higher current densities along with longer stability. The descriptive analysis involving the designing strategies of the binder-free catalysts over 3D frameworks, their physical viability, and their

P.D. Patel Institute of Applied Sciences, Charotar University of Science and Technology, CHARUSAT, Anand, Changa, Gujarat-388421, India. E-mail: cksuresh.cv@charusat.ac.in



performance have been included in this review. We have also discussed the factors that hinder the growth of current density and ongoing operational strategies to overcome them.

## 2 Electrode/electrolyte design configurations for high current density water electrolysis system

The three main electrolyzer methods are elaborated in Table 1 are frequently used for water splitting are Alkaline Water

Electrolysis (AWE), Proton Exchange Membrane Water Electrolysis (PEMWE), and Alkaline Exchange Membrane Water Electrolysis (AEMWE) Fig. 1. To effectively go from lab-scale configurations, these systems must be modified under carefully monitored operating conditions. Chen *et al.* have addressed common factors that hinder the commercialization of these electrolyzers. These parameters include ohmic losses with increasing current, and disturbed gas management leads to poor mass transport and uneven current distribution. Moreover, the degradation of catalysts due to high potentials

**Table 1** The technical parameters for AWE, PEMWE, and AEMWE to achieve high current density and commercial durability are described here<sup>11,12</sup>

Parameter	AWE	PEMWE	AEMWE
Electrolyte	KOH (20–30%)	Pure water	Alkaline solution (dilute)/pure water
Working temperature °C	(60–90)	(50–80)	(40–70)
Current density ( $\text{mA cm}^{-2}$ )	<0.5	1–2	1–2
Membranes	Diaphragm	Proton exchange membrane	Anion exchange membrane
Electrocatalysts	Ni, NiFeO <sub>x</sub>	Platinum-based/IrO <sub>x</sub> , RuO <sub>x</sub>	PGM-free
Local pH	Alkaline	Acidic	Alkaline
Expected cost	Low	High	Targeting low

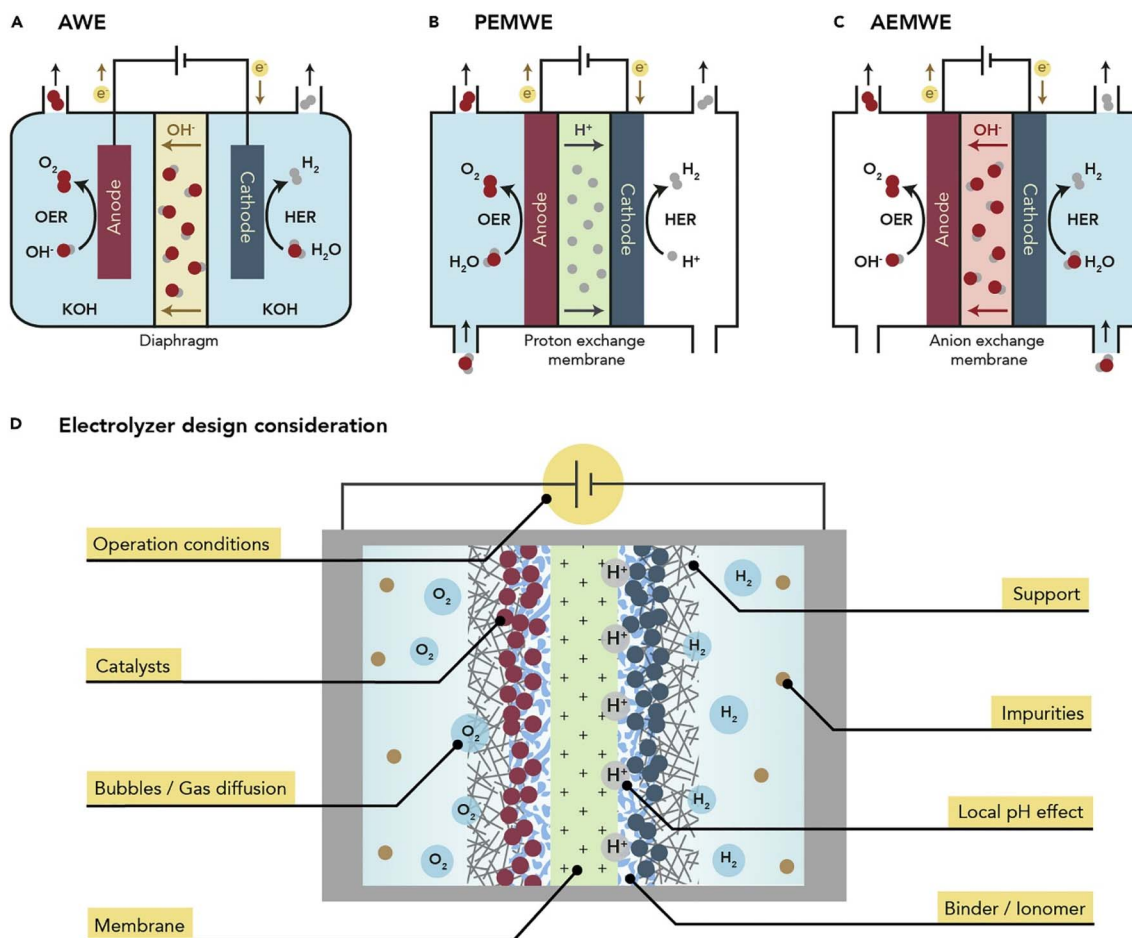


**Fig. 1** Water electrolysis system electrode/electrolyte design configurations: (a) alkaline water electrolyzers (AWE), (b) proton exchange membrane water electrolyzers (PEMWE), (c) alkaline exchange membrane water electrolyzers (AEMWE), (d) key strategies influencing water electrolyzers with for operating in high current density and long-term stability. Reproduced from ref. 10. Copyright the Cell Press, 2021.



invites unwanted material breakdown and degraded performance.<sup>10</sup>

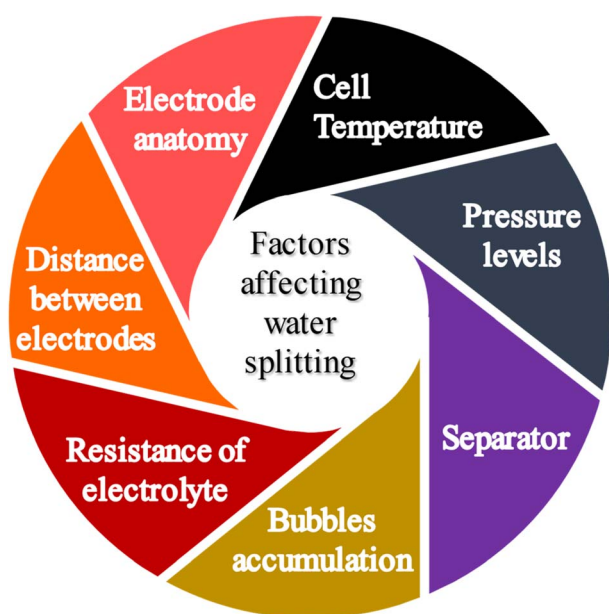
According to Sun *et al.*, the benefits of employing alkaline water electrolyzers include high hydrogen production, a concise design, and minimal resistance loss. In discussing PEMWE, the combination of the membrane and electrode not only enhances performance but also regulates the liquid–gas flow. The merger of AWE and PEMWE has led to the establishment of AEMWE, which utilizes electrolysis in an alkaline medium and structures the solid polymer electrolyte to address leakage issues. Sun *et al.* also acknowledged the advancement of industry-relevant catalyst designs alongside cost management, stating that a practical approach can connect laboratory-scale work to the industrial production of hydrogen<sup>12</sup>

### 2.1 Electrode material and catalyst selection for high current density electrolyzer

The recent research on high current density water electrolysis ought to concentrate on fine-tuning crucial elements that greatly impact energy efficiency and cell performance. Some of these elements are mentioned in Scheme 1, which should be kept in mind before selecting the electrode material. These parameters also support in bifurcation of electrode material based on the electrochemical applications. (1) Thermal management upgrades the performance of the electrochemical cell by reducing the degradation of the catalyst. Addressing this, researchers should study sophisticated thermal management approaches to decrease temperature-induced inefficiencies. Similar to this, the liquid water flow rate increases the reactant supply and gas removal up to a point where benefits start to wane. (2) Future studies should seek to discover ideal operating pressure levels that decrease the stress on the material caused by the excessive production of hydrogen. This also affects the

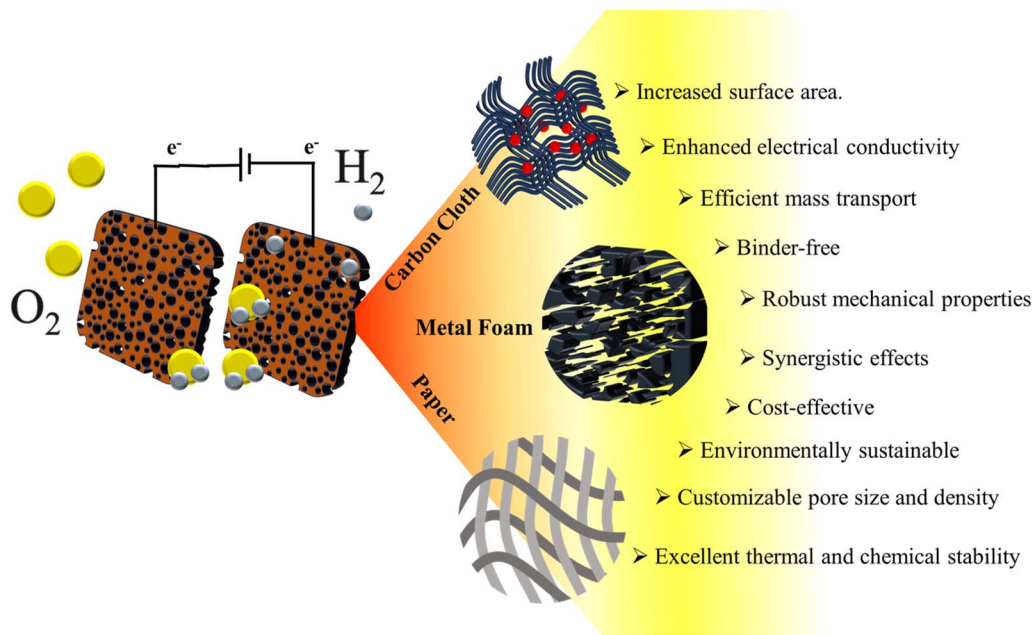
active surface area of the electrode, leading to a decrease in the system's performance. (3) The selection of a separator/diaphragm is a crucial step as it withstands both chemical and thermal stress. Additionally, an increase in the flow of ionic charges and prevention of the mixing of gas incredibly support the electrolyzer's efficiency at the commercial level. (4) Controlling gas accumulation is still important since higher temperatures and ohmic resistance make this problem worse by blocking active sites, which lowers efficiency. Innovative designs, such as porous electrode materials anchored with hydrophilic surfaces, can reduce gas and provide a uniform current distribution. (5) Moreover, solution resistance plays a significant role in elevating the current density. The number of ionic carriers in the electrolyte encourages the easy flow of current by reducing the resistance and supporting the higher conductivity. These can also be reduced by maintaining the appropriate distance between the electrodes. The distance among the electrodes plays a vital role in managing the voltage drop and lower mass transport. (6) The electrode anatomy has been the most researched topic in the last few decades because connecting the lab-scale work to commercial conditions requires electrode species that can withstand harsh conditions. Industrial electrolyzers often require  $>500 \text{ mA cm}^{-2}$  current densities for the generation of hydrogen and oxygen gas. However, this leads to wear-out of the catalyst's material after an extended period due to the excessive formation of bubbles on the cathode–anode interface, restricting the intrinsic activity, and the corrosion effect due to the highly alkaline medium. Interestingly, researchers have reported various non-noble electrocatalysts based on their design technique, among which powdered-based catalysts have shown outstanding results at the laboratory scale, but these electrodes lack durability and efficiency when employed at large production houses due to their degradation in terms of both efficiency and survival. To overcome this, self-supported binder-free electrocatalysts have made their mark in mass hydrogen production. These electrodes not only lower the production cost by eliminating the requirement of binder or adhesion but also directly grow catalysts on the supporting substrate, prolonging the life cycle of the electrocatalysts. Moreover, the space between the 3D arrays provides space for the penetration of ions that can lead to faster adsorption and desorption of gases. Additionally, the powdery electrocatalysts are post-coated on the substrates, which might result in the wear-out of layers when exposed to multiphase reactions. In the case of self-supported electrocatalysts, the material is tightly bound within the substrate, which favors the high mechanical stability for multiple desired periods.<sup>13</sup> Direct contact prioritizes the electrode/electrolyte interface activities by reducing the charge transfer resistance and by providing a higher enlarged active surface area.<sup>13,14</sup>

The selection of substrate plays a vital role in lowering the overpotential by forming a synergistic effect with the loaded catalyst material, which is essential for exposing a higher number of active sites for a higher electron transfer mechanism. Scheme 2 showcases some of the actively used substrate materials, such as carbon cloth, metal foams, and cellulose paper, and their efficiency for being chosen for the evaluation at



Scheme 1 Factors affecting high current density water electrolysis.





Scheme 2 Advantages of fabric and foam-based heterostructure catalysts for electrocatalytic hydrogen production.

higher current density. All of these substrates hold a specialty in terms of conductivity, mechanical and electrical strength, and survival rate in the electrolyte system. Keeping this in mind, the performance optimization of the electrocatalysts is done.

Enhanced strength and flexibility are observed in carbon-based substrate materials and cellulose paper electrodes. They also provide higher electron conductivity, which enables the flow of ions, successively increasing the catalytic performance. Sharma *et al.* presented an innovative method to transform ordinary cotton-polyester fabric into a flexible catalytic current collector for water and urea electrolysis aimed at industrial-scale hydrogen production, addressing energy and environmental sustainability challenges. The electroactive sites present in the interfacial spaces between the fabric provide bridges for the transportation of electrons subconsciously increasing the catalytic activity. The NiP-fabric electrodes demonstrated outstanding HER performance across various environments, achieving overpotential values of 159 mV in alkaline, 127 mV in acidic, and 94 mV in artificial seawater at a current density of 10 mA cm<sup>-2</sup>.<sup>15</sup> In addition to the fabric material, carbon cloth has made its way to industrialization due to its excellent porous structure and electrical–mechanical strength. The carbon fiber allows vivid electron configurations with the catalyst material ensuring longer durability and stability for a longer period. The study of enhanced minimal resistance supporting higher charge transport of carbon cloth was done by Chauhan *et al.* by synthesizing NiCo-LDH@MoS<sub>2</sub>/CuS heterostructure on it. The results claim the multi-use of 3D electrodes for electrochemical applications. The catalyst material was held in the interstices of the carbon fibres, withstanding the industrial current density for an extended time. The work significantly elaborates on the property of a self-supported electrocatalyst directly grown on carbon cloth using a single-step hydrothermal method.

Moreover, the asymmetric study for the supercapacitor performance reveals the fact that carbon cloth holds a remarkable position in the field of flexible electronics.<sup>16</sup>

Although carbon cloth has numerous advantages, the degradation of the anode is due to the vigorous oxidation reactions with increasing current densities. Therefore, metal-foam-based electrodes provide interlinked network-generating pathways for ion species to interact with the electrolyte. Additionally, active sites generated during electrocatalytic reactions improve the overall performance. Chauhan *et al.* synthesized Fe<sub>2</sub>B/MXene directly on nickel foam using a chemical reduction technique for the evaluation of the overall water-splitting mechanism. The electrocatalyst displayed tremendous stability at high current density, and eventually, the increased active number of sites is due to the synergistic effect formed between the metal borides and metal oxides.<sup>17</sup> Shao *et al.* fabricated a porous Cu–Ni/Ni–Cu alloy within a nickel foam, substantially improving the number of reactive sites for the liberation of adsorbed hydrogen. The study also revealed an outstanding overpotential of 31 mV at 10 mA cm<sup>-2</sup>, which is much lower compared to that of the commercial platinum electrode. This marks the footprint of improved catalysis using a porous 3D substrate.<sup>18</sup> Table 2 showcases electrocatalysts anchored with various 3D substrates to evaluate their HER, OER, OWS, and UOR performance, durable at high current densities for long periods.

Fig. 2 depicts different substrates withstanding high current density when decorated with a variety of transition metal-based nano materials. Shah *et al.* developed a nickel-based composite, specifically self-supported Mn-doped Ni<sub>3</sub>Se<sub>2</sub> electrocatalysts, for water and urea electrolysis aimed at energy-saving hydrogen production. In Fig. 2(a), the lattice distortion intentionally enhanced the adsorption and desorption of hydrogen atoms



Table 2 Cutting-edge electrocatalysts embedded in various 3D frameworks with high current density and commercial durability<sup>a</sup>

Electrocatalysts	Matrix	Medium	Reactions performed	Current density (mA cm <sup>-2</sup> ) achieved	Robustness (h @ mA cm <sup>-2</sup> )
Cr doped FeNi <sub>3</sub> /NiFe <sub>2</sub> O <sub>4</sub> (ref. 19)	Ni foam	Alkaline	HER/OER/OWS	1000	200 @ 1000
NiCoMn <sup>20</sup>	Ni foam	Alkaline	HER/OER/OWS	1000	300 @ 100
Fe <sub>2</sub> B/MXene@NF <sup>17</sup>	Ni foam	Alkaline	HER/OER/OWS	400	80 @ 300
CuCoSnO <sub>x</sub> (ref. 21)	Ni foam	Alkaline	HER/OER/UOR/OWS	400	48 @ 300
Mn/NiBP <sup>22</sup>	Ni foam	Alkaline	HER/OER/OWS	2000	120 @ 1000
Pt-MoS <sub>2</sub> -Co@CHNF <sup>23</sup>	Cu foam	Alkaline	HER	500	24 @ 500
Co-MOF(ZIF-67) <sup>24</sup>	Poplar wood	Alkaline	HER	500	50 @ 10
FeCoCuS <sub>x</sub> /CF <sup>25</sup>	Co Fe foam	Alkaline	HER	1000	100 @ 100
PdRu@Mo <sub>x</sub> (ref. 26)	Ni foam	Alkaline	HER	1000	10 @ 1000
Cu-Ni-MoS <sub>2</sub> (ref. 27)	Carbon cloth	Alkaline	HER	500	20 @ 500
Ni <sub>3</sub> S <sub>2</sub> /Cr <sub>2</sub> S <sub>3</sub> (ref. 28)	Ni foam	Alkaline	HER	1000	50 @ 500
h-NiMoFe <sup>29</sup>	Ni foam	Alkaline	HER	1000	10 @ 1500
NiFe-P@NC <sup>30</sup>	Ni Fe foam	Alkaline	HER/OER/OWS	500	12 @ 500
NC/Ni <sub>3</sub> Mo <sub>3</sub> N <sup>31</sup>	Ni foam	Alkaline	HER	1100	50 @ 1100
Ni <sub>2</sub> P/NiMoP <sup>32</sup>	Ni foam	Alkaline	HER/OER/UOR/OWS	500	80 @ 10
NC/NiNPs <sup>33</sup>	Glassy carbon electrode	Alkaline	HER	1400	260 @ 1400
RuFe-Ni <sub>2</sub> P <sup>34</sup>	Ni foam	Sea water	HER/HzOR/OH <sub>2</sub> S	1000	100 @ 1000
Cu NWs@NiFe-Pt <sub>3</sub> Ir <sup>35</sup>	Cu foam	Alkaline	HER	500	7 days @ 500
Ru/CuMnBP <sup>36</sup>	Ni foam	Alkaline	HER/OER/OWS	2000	10 @ 2000
NiFeOOH@NiFe/Ni <sup>37</sup>	Ni mesh	Alkaline	HER/OER/OWS	1000	100 @ 500
FCN-MOF <sup>38</sup>	Ni foam	Alkaline	OER	1000	50 @ 1000
MoS <sub>2</sub> /Mo <sub>2</sub> C <sup>39</sup>	Pt foil	Alkaline	HER	1000	24 @ 200
MnO <sub>x</sub> /NiFeP <sup>40</sup>	Ni foam	Alkaline	HER/OER/OWS	1000	70 @ 1000
Ni(OH) <sub>x</sub> /Ni <sub>3</sub> S <sub>2</sub> (ref. 41)	Ni foam	Alkaline	HER	1000	1000 @ 1000
F-Co <sub>2</sub> P/Fe <sub>2</sub> P <sup>42</sup>	Iron foam	Alkaline	HER	3000	10 @ 2000
FeNiO <sup>43</sup>	Ni foam	Alkaline	HER/OER/UOR/OWS	400	20 @ 300
CuCo <sub>2</sub> S <sub>4</sub> (ref. 44)	Ni foam	Alkaline	HER/OER/UOR/MOR/OWS	300	72 @ 25
Cu <sub>2</sub> CoSnS <sub>4</sub> (ref. 45)	Whatman filter paper	Acidic, alkaline, neutral	HER	700	118 @ 0.3V vs. RHE
TS-NiFe LDH <sup>46</sup>	Ni foam	Alkaline, alkaline seawater	HER, OER, OWS	1000	350 @ 1000

<sup>a</sup> HER: hydrogen evolution reaction; OER: oxygen evolution reaction; UOR: urea oxidation reaction; HzOR: hydrazine oxidation reaction; OH<sub>2</sub>S: overall hydrazine splitting; OWS: overall water splitting; MOR: methylene blue oxidation reaction

(H\*) on the active sites. Additionally, the direct growth of nickel foam contributes to a synergistic effect, reducing charge transfer resistance. The manganese Mn-doped Ni<sub>3</sub>Se<sub>2</sub> exhibited remarkable chemical stability, ensuring excellent long-term performance, which is essential for practical applications. The multivalency of Mn improves the overpotential by accelerating mass diffusion at the electrode interface. In a two-electrode electrolyzer, the system achieved low cell voltages of 2.02 V for water electrolysis and 1.77 V for urea electrolysis to generate a current density of 100 mA cm<sup>-2</sup>, showcasing its potential for efficient hydrogen generation.<sup>47</sup> Fig. 2(b) is the detailed study of vanadium-doped Cu<sub>2</sub>S nano catalyst for the evaluation of HER and OER performance. Sharma *et al.* directly synthesised the electrocatalyst on copper foam using the hydrothermal technique. It is noted that the vanadium doping increases the ionic interaction by forming the electron density around the Cu-sites, which is essential for improved HER and OER. Moreover, the porous structure enables electron transport by lowering the charge transfer resistance and improving the mass transport mechanism.<sup>48</sup> Trivedi *et al.* reported a one-step hydrothermal

synthesis of bifunctional Cr-Cu<sub>2</sub>S nanoflakes supported on copper foam (Cr-Cu<sub>2</sub>S@CF) for use in alkaline water electrolyzers aimed at industrial-scale hydrogen production Fig. 2(c). The study displays the change in the electronic structure of Cu<sub>2</sub>S after the incorporation of Cr as a dopant, which leads to enhanced HER performance. The vertically oriented Cr-Cu<sub>2</sub>S nanoflakes form a hierarchical network providing the electrochemical active surface area of about 3525 cm<sup>2</sup>. The formation of Cr<sup>3+</sup> electron density around the Cu<sup>+</sup> sites enhances electrocatalytic activity by faster adsorption and desorption of the ions. Hence, the advanced morphological features and binder-free electrocatalytic performance of Cr-Cu<sub>2</sub>S@CF for both HER and OER at high current densities are suitable for industrial applications.<sup>49</sup>

Frederiksen *et al.* designed a customized electrolyzer cell developed by Advanced Surface Plating, capable of operating under industrial-relevant conditions, as shown in Fig. 2(d). The aim was to link the lab-based development to the industrial scale.<sup>50</sup>



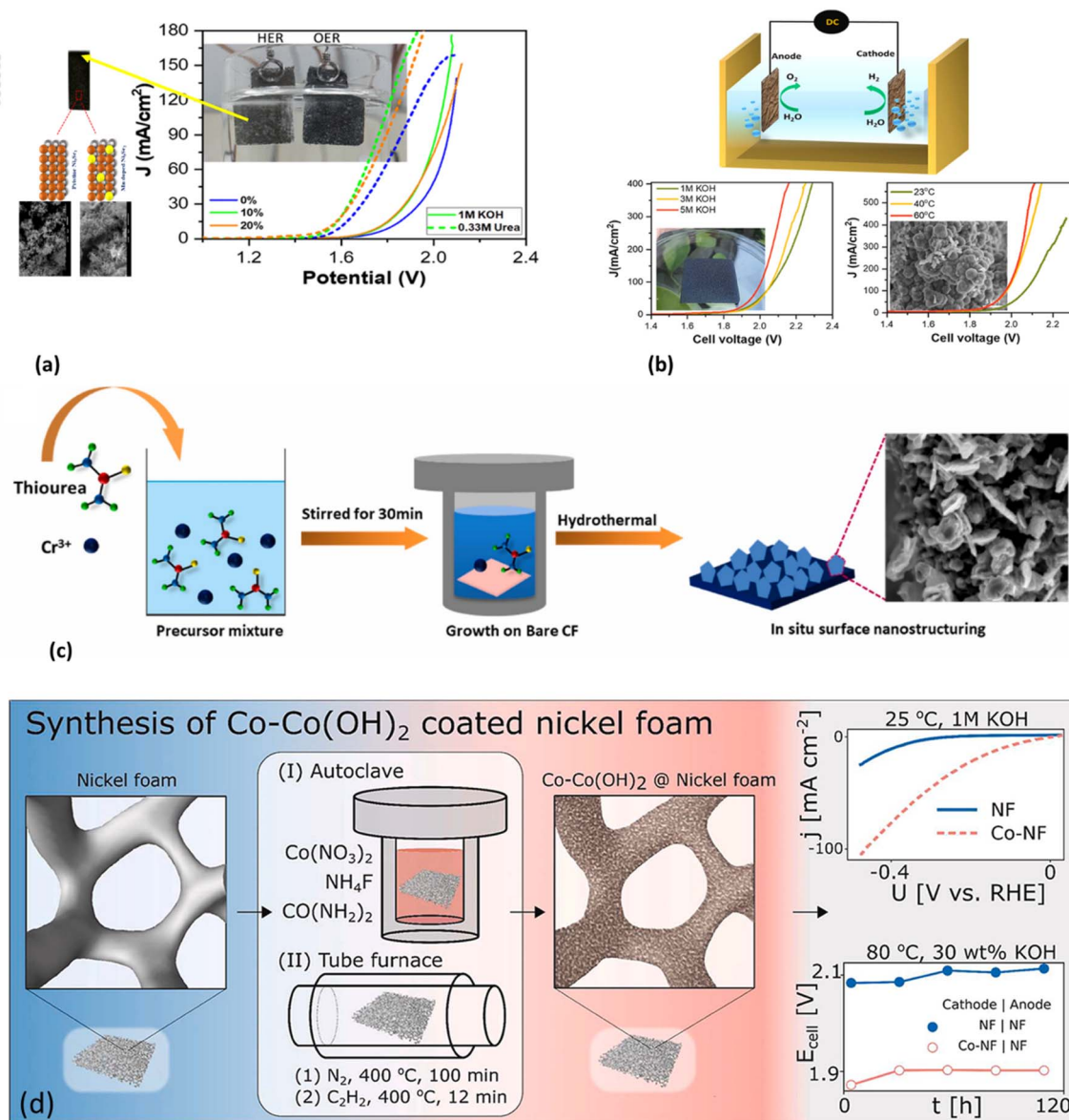
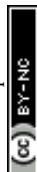
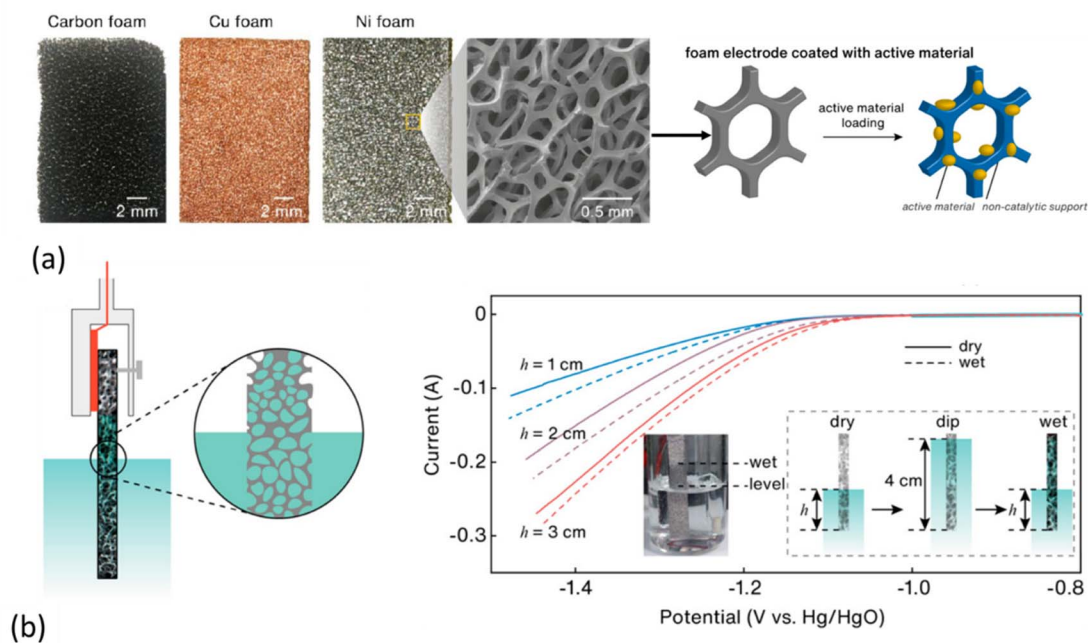


Fig. 2 (a) Nanostructured Mn-Ni<sub>3</sub>Se<sub>2</sub>@NF acts as an electrocatalyst for overall water splitting. Reproduced with permission from ref. 47 copyright ACS Applied Materials & Interfaces, 2024. (b) Self-supported V-Cu<sub>2</sub>S@CF (copper foam) electrode for green hydrogen production through alkaline water electrolysis. Reproduced with permission from ref. 48 copyright International Journal of Hydrogen Energy, 2024. (c) Cr-Cu<sub>2</sub>S Nanoflakes supported on Cu-foam (Cr-Cu<sub>2</sub>S@CF) for alkaline water electrolyzer for H<sub>2</sub> production at an industrial scale. Reproduced with permission from ref. 49 copyright International Journal of Hydrogen Energy, 2024. (d) electrolysis cell for testing at industrial conditions: Co-Co(OH)<sub>2</sub>/NF electrolyzer tested at industrial conditions. Reproduced with permission from ref. 50 copyright International Journal of Hydrogen Energy, 2024.

The catalyst-anchored, Ni-foam, self-supported electrode demonstrated a reduction in cell potential by 200 mV at a current density of 200 mA cm<sup>-2</sup>, sustaining performance for over 118 h of electrochemical testing at 80 °C in a 30 wt% KOH electrolyte.<sup>50</sup> One of the most important aspects of developing water electrolysis for the creation of green hydrogen is material selection, particularly when large current densities are involved. To guarantee effective and long-lasting performance, the materials selected for catalysts, membranes, and other electrolyzer components must balance activity, durability, and cost. Because of the improved electrode distribution made possible

by the larger surface area, each site's local current density is decreased. The kinetics of the evolution reactions of hydrogen and oxygen are enhanced as a result, as there is less burden on each reaction site, which minimizes energy loss from overpotentials. Gui *et al.* developed a one-step electrodeposition process to synthesize NiFePS on carbon cloth (CC) to create self-supported electrodes for total water splitting. There were two main reasons for these electrodes' remarkable electrocatalytic activity. First, the high conductivity of the carbon cloth reduces charge transfer resistance between the electrode and electrolyte, improving electron transfer rates by acting as an efficient





**Fig. 3** (a) Digital pictures of three common open-pore foam-type electrodes, including carbon, copper, and nickel, together with an SEM image of Ni foam and a schematic of catalyst-embedded Ni foam. (b) Schematic representation of electrolyte filling the pores of a foam-type electrode due to capillary action. HER polarization curves for “dry” (solid line) and “wet” (dotted line) Ni foam electrodes in 1.0 M KOH. Together with an illustration of the “wet” electrode, the preparation procedures for both “dry” and “wet” Ni foam electrodes are also displayed. Reproduced with permission from ref. 53. Copyright ACS Applied Materials & Interfaces, 2024.

growth substrate. Second, the electrochemical surface area of the catalyst is increased by the ultra-thin nanosheets that grow on its surface, which offer more active reaction sites and increase the catalytic efficiency overall.<sup>51</sup> Liu *et al.* synthesized ultra-small ruthenium-nickel alloy nanoparticles, stably anchored on reduced graphene oxide papers (Ru-Ni/rGOPs), as versatile electrocatalysts for the HER in acidic and alkaline environments. The self-supported hybrid electrode demonstrated an impressively low overpotential of approximately 106 mV to achieve a current density of 1000 mA cm<sup>2</sup> while maintaining excellent stability for over 1000 h in 1 M KOH.<sup>52</sup> Kuang *et al.* produced cobalt-nickel-iron phosphides (CoNiFeP) on Ni foam (NF) using a simple one-step electrochemical deposition method, creating self-supported electrodes for efficient water splitting.

Zheng *et al.* claimed that the 3D porous metal frames Fig. 3(a) allow easy passage of electrolyte and gas, acknowledge the high specific surface area, and hold the loaded catalyst material firmly for the electrochemical process at high current density. They studied various aspects of metal frames, which might be problematic for utilizing the 3D electrodes at a large scale. One of such is the capillary effect, where in Fig. 3(b), the metal foam is partially dipped; however, the few mm of porous foam above the electrolyte also takes part in the chemical reaction by absorbing liquid molecules. This can subconsciously disturb the current density study. To address these issues, scientists have utilized the method of plugging epoxy glue in the pores of foams. Moreover, Zheng *et al.* studied this effect by dipping different lengths of the Ni foam into 1 M KOH,

to which vivid current responses were recorded. The one that was first completely immersed in the electrolyte and then suspended at a particular length showed increased current density owing to the more active sites compared to the partially dry electrodes. Additionally, the type of catalyst loading also affects the current density. Hence, the troubleshooting of problems arising from the experimental setups can increase the survival and competence rate of 3D frames at commercial levels.<sup>53</sup>

The high catalytic performance was attributed to the formation of 3D spherical clusters by introducing Fe into CoNiP, which increased the number of active sites and enhanced gas diffusion. Furthermore, surface reconstruction into metal oxides/hydroxides synergistically improved the intrinsic activity of CoNiFeP. The prepared catalysts demonstrated excellent durability, remaining stable for 100 h even at a high current density of 50 mA cm<sup>-2</sup>.<sup>54</sup> Mo *et al.* produced a novel self-supported nickel-iron foam covered with Ni<sub>2</sub>B particles through a solid-phase boronization method called NFF-B. This bi-functional setup for overall water splitting required only 1.49 V to drive electrolysis at 10 mA cm<sup>-2</sup> and maintained exceptional stability for 115 h, surpassing most previously reported bifunctional electrocatalysts. The enhanced activity and durability were attributed to the high conductivity of the NFF-B substrate, the synergistic effect with Co-doped NiSe, the optimized electronic structure from Co-doping, and the petal-shaped nanosheets that provided more active sites.<sup>55</sup>

The electrolyzer is the main element of a water electrolysis system, which is where the actual water splitting takes place. An anode, or positive electrode, and a cathode, or negative



electrode, make up the electrolyzer. Water is oxidized at the anode to release protons, electrons, and oxygen gas. Electrons at the cathode reduce protons to create hydrogen gas. The results of the investigations demonstrated how important self-supported electrodes are to obtaining high current density in water electrolysis. Self-supported designs with high conductivity and expanded electrochemically active surface area, like cobalt-nickel-iron phosphides and nickel-iron foam covered with novel catalysts, showed improved catalytic performance. To preserve stability and performance at high current densities, these characteristics reduced charge transfer resistance and promoted effective mass transport. Self-supported electrodes have the potential to outperform conventional electrocatalysts, as demonstrated by these examples of sustained operation over extended periods. This makes them essential for the advancement of water-splitting technologies and the promotion of sustainable energy solutions.

## 2.2 Electrolyte selection for high current density water electrolysis

In water electrolysis systems, choosing the right electrolyte and membrane is essential to maximizing durability, performance, and efficiency. These elements impact ionic conductivity, reaction kinetics, and system stability. The alkaline water

electrolyzers (AWE) are the most historic way of large-scale green hydrogen production. The cost to produce hydrogen per kg using AWE is estimated to be \$2 to \$3. The system employs two electrodes immersed in the highly concentrated electrolyte, which can be either potassium or sodium hydroxide. The porous oxide diaphragm is appointed for the exchange of  $\text{OH}^-$  ions between the electrode and also bifurcates the  $\text{H}_2$  and  $\text{O}_2$  gases produced on the cathode and anode, respectively. However, the electrolyte concentration plays a vital role in uplifting the functions of the AWE, as it enhances the production of hydrogen by encouraging the chemical reactions. The conducting electrolytes, such as KOH and NaOH, are responsible for the availability of  $\text{OH}^-$  ions essential for the generation of hydrogen gas. Apart from this, researchers have also shown great interest in evaluating other highly alkaline electrolytes such as LiOH,  $\text{Ba}(\text{OH})_2$ ,  $\text{K}_2\text{CO}_3$ , and many more. Potassium Hydroxide (KOH) is widely employed in alkaline water electrolysis because of its high ionic conductivity and stability in alkaline settings, and better conductivity.<sup>43,47,56</sup> Typical concentrations of KOH range from 20% to 40% by weight. The selection of the electrolyte affects critical parameters, including temperature stability (alkaline electrolytes frequently function at high temperatures up to 90 °C to improve reaction kinetics) and ionic conductivity, which is essential for reducing ohmic losses and optimizing system efficiency.<sup>45,56</sup> To guarantee

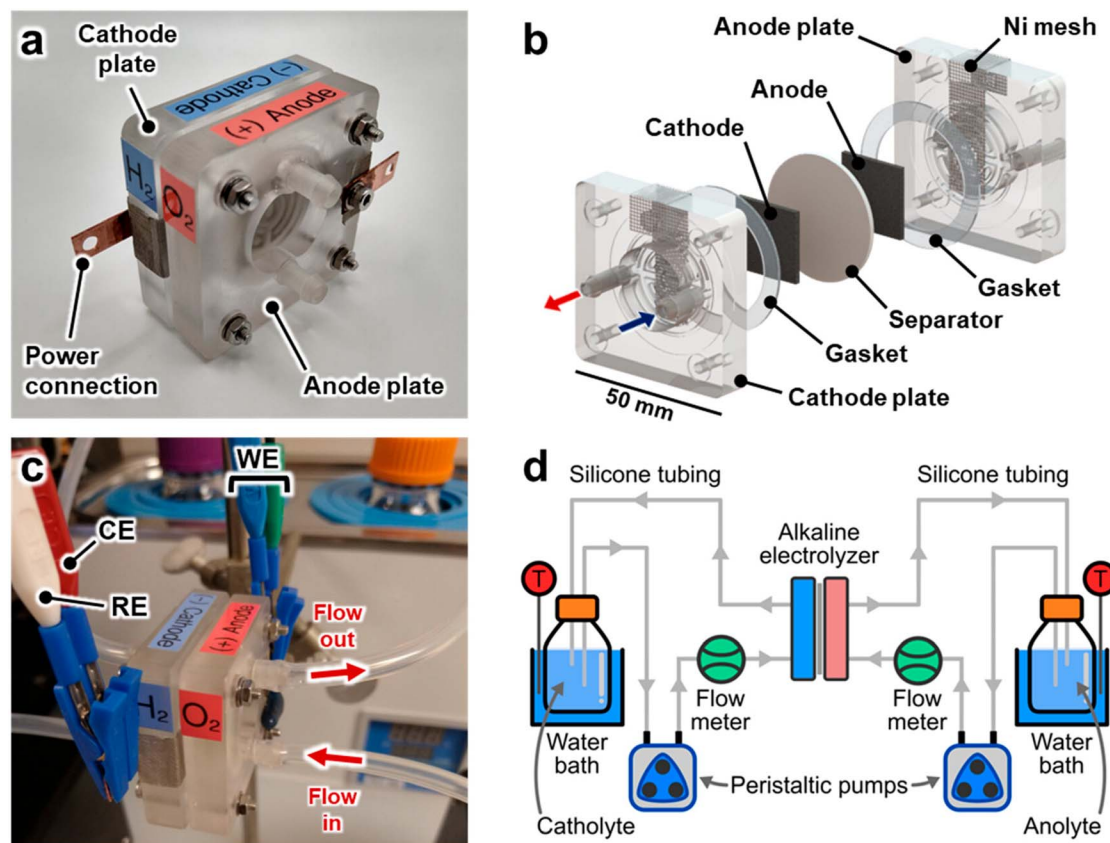


Fig. 4 Flow electrolyzer setup for lab-scale electrocatalyst testing: (a) fully assembled electrolyzer cell, (b) exploded view illustrating the electrolyzer and its components, (c) electrolyzer in operation, and (d) process flow diagram of the electrolyzer system. Reproduced with permission from ref. 57 copyright ACS Energy Letters, 2024.



dependable and effective functioning, the electrolyte must preserve stability and withstand heat degradation under these circumstances.

For the practical scale applications, evaluation of the model at the lab scale is essential. Therefore, Marquez *et al.* in Fig. 4 proposed a zero-gap configuration with realistic AWE conditions to predict criteria and protocols that can help to optimise the conditions for the commercialization of lab-employed experiments. They designed a prototype where the continuous flow of electrolytes was performed for bubble management. Also, the temperature of the electrolyte was maintained using a water bath, which helped in the detailed analysis of the behavior of the electrolyzer in the presence of different temperatures and at various concentrations. The results suggest that managing the temperature, electrolyte concentration, and gas accumulation can soften the route to survive a lab-scale electrolyzer at commercial scale.<sup>57</sup>

Before employing the lab-prototypes, the compatibility of the electrode along the electrodes needs to be identified. Therefore, Fig. 5 displays vivid types of electrolytes, and the effect of temperature is analysed for different catalyst materials anchored to various 3D frameworks. For instance, Sharma *et al.* reported the synthesis of  $V_xNi_{1-x}O$  catalysts supported on a three-dimensional Ni-foam scaffold for catalytic water and urea electrolysis, as illustrated in Fig. 5(a)–(c). The self-supported 3D architecture significantly increased the catalyst's surface area, exposing numerous electrocatalytically active sites. The  $V_xNi_{1-x}O$  catalysts demonstrated exceptional HER, OER, and UOR performance, driven by the incorporation of

vanadium, which reduced interfacial resistance, enhanced electrochemical surface area, and accelerated reaction kinetics. The electrode was also tested at different temperatures ranging from 20 °C to 60 °C. With increasing temperature, an improvement in the overpotential is noted, which can be attributed to faster ionic diffusion. The catalyst required 2.01 V in 1 M KOH to achieve the current density of 100 mA cm<sup>-2</sup>, which was reduced to 1.74 V to achieve 100 mA cm<sup>-2</sup> in 1 M KOH + 0.33 M Urea. Due to the formation of the NiOOH phase, the number of active sites increases, which significantly reduces the OER overpotential by 266 mV for the urea oxidation reaction. Stability was assessed with a current density of 20 mA cm<sup>-2</sup> for 70 h during water electrolysis, and 100 mA cm<sup>-2</sup> for 67 h during urea electrolysis.<sup>56</sup> Rezaee *et al.* reported the development of a cMOF/LDH heterostructure, self-supported on carbon cloth, as an efficient conductive support for enhanced electron transport, improved catalytic sites, and superior electrocatalytic activity for overall water splitting, as shown in Fig. 5(d). Electrocatalyst displayed the excitingly low overpotentials of 49 mV and 230 mV to achieve the current density of 10 mA cm<sup>-2</sup> for HER and OER, respectively, in alkaline electrolyte. The factors responsible for the excellent performance of work highlight the benefits of 3D-network-based conducting substrates in promoting efficient and sustainable electrochemical processes.<sup>58</sup> Liu *et al.* presented a “one for two” strategy in which a cobalt-based metal-organic framework array-derived CoFeNi-layered double hydroxide anode and CoP/FeNi<sub>2</sub>P heterojunction cathode for an alkaline seawater electrolyzer. The CFN-LDH/NF displayed an overpotential of 352 mV

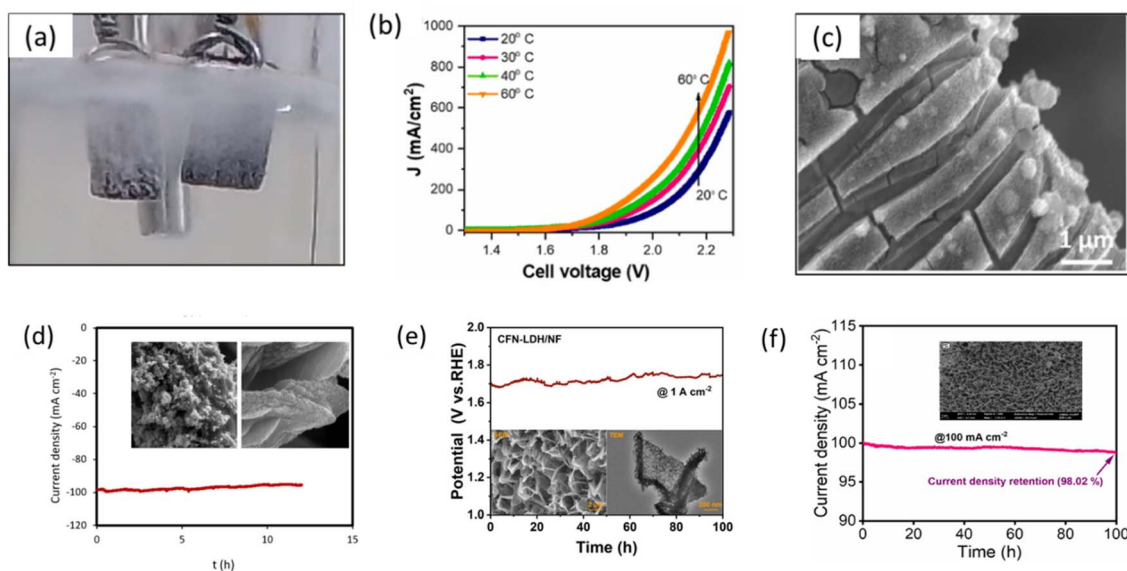


Fig. 5 (a–c) Digital image of alkaline water electrolyzer, (b) LSV polarization curves of  $V_{0.10}Ni_{0.90}O/NF$  in 1.0 M KOH at various temperatures ranging from 20 to 60 °C, (c) SEM images of  $V_{0.10}Ni_{0.90}O@NF$  after stability testing at 1000 mA cm<sup>-2</sup> in 1.0 M KOH. Reproduced with permission from ref. 56 copyright International Journal of Hydrogen Energy, 2024, (d) cMOF/LDH hetero-nano petals decorated with metal-N sites shelled over WNO nanowire show superior bifunctional activity with stability and post-stability measurements. Reproduced with permission from ref. 58 copyright Journal of Colloid and Interface Science, 2024, (e) CFN-LDH/NF at 1 A cm<sup>-2</sup> current density with SEM and TEM of CFN-LDH/NF after 100 h stability test. Reproduced with permission from ref. 59 copyright 2024 Journal of Colloid and Interface Science, 2024, (f) chronoamperometric stability of the  $Co_2P-VP@N-C/Co$  device for 100 h at 100 mA cm<sup>-2</sup> with post stability SEM image. Reproduced with permission from ref. 60 copyright Journal of Colloid and Interface Science, 2024.



Table 3 Comparison of different electrodes in different electrolytes

Electrocatalysts	Electrolytes	Overpotential for HER at $\eta$	Overpotential for OER/UOR at $\eta$	Cell potential at $\eta$	Durability
$V_xNi_{1-x}O^{56}$	1 M KOH	175 mV at $\eta_{10}$	1.684 V at $\eta_{100}$	1.7 V at $\eta_{10}$	17 h at $\eta_{1000}$
	1 M KOH + 0.33 M urea		1.34 V at $\eta_{100}$	1.53 V at $\eta_{10}$	67 h at $\eta_{100}$
RuCoFe-NPs@WNO-NWs <sup>58</sup>	1 M KOH	49 mV at $\eta_{10}$	230 mV $\eta_{10}$	1.49 V at $\eta_{10}$	12 h at $\eta_{10}$
	Alkaline seawater			1.55 V at $\eta_{10}$	
CFNP/NF  CFN-LDH/NF <sup>59</sup>	1 M KOH	281 mV at $\eta_{1000}$	352 mV at $\eta_{1000}$	1.71 V at $\eta_{100}$	100 h at $\eta_{1000}$
	Alkaline seawater	312 mV at $\eta_{1000}$	392 mV at $\eta_{1000}$	1.791 V at $\eta_{100}$	100 h at $\eta_{500}$
Co <sub>2</sub> P-VP@N-C/Co (+, -) <sup>60</sup>	1 M KOH	68 mV at $\eta_{10}$	280 mV at $\eta_{30}$	1.49 V at $\eta_{10}$	100 h at $\eta_{100}$
Co-Ni <sub>3</sub> S <sub>2</sub> /NF <sup>61</sup>	1 M KOH		340 mV at $\eta_{100}$		
	1 M KOH + seawater		368 mV at $\eta_{100}$		50 h at $\eta_{500}$
Ni <sub>3</sub> S <sub>2</sub> foam/NF <sup>62</sup>	1 M KOH		329 mV at $\eta_{100}$		
	1 M KOH + seawater		369 mV at $\eta_{100}$		1000 h at $\eta_{500}$
NCP/PC and NCP/PC  DSA <sup>63</sup>	1 M KOH + seawater	92 mV at $\eta_{100}$			1000 h at $\eta_{1000}$
	1 M KOH + seawater			2.65 V at $\eta_{200}$	150 h at $\eta_{500}$
	1 M KOH + seawater				

to gain the current density of 1000 mA cm<sup>-2</sup> in 1 M KOH due to the synergistic effect of tri-metal. Moreover, CFNP/NF was evaluated for the HER performance, where it attained the 1000

mA cm<sup>-2</sup> with the lower overpotential of 281 mV in 1 M KOH. The overall activity of CFN-LDH/NF||CFNP/NF in alkaline seawater predicted the lower cell voltage of 1.791 V at 100 mA

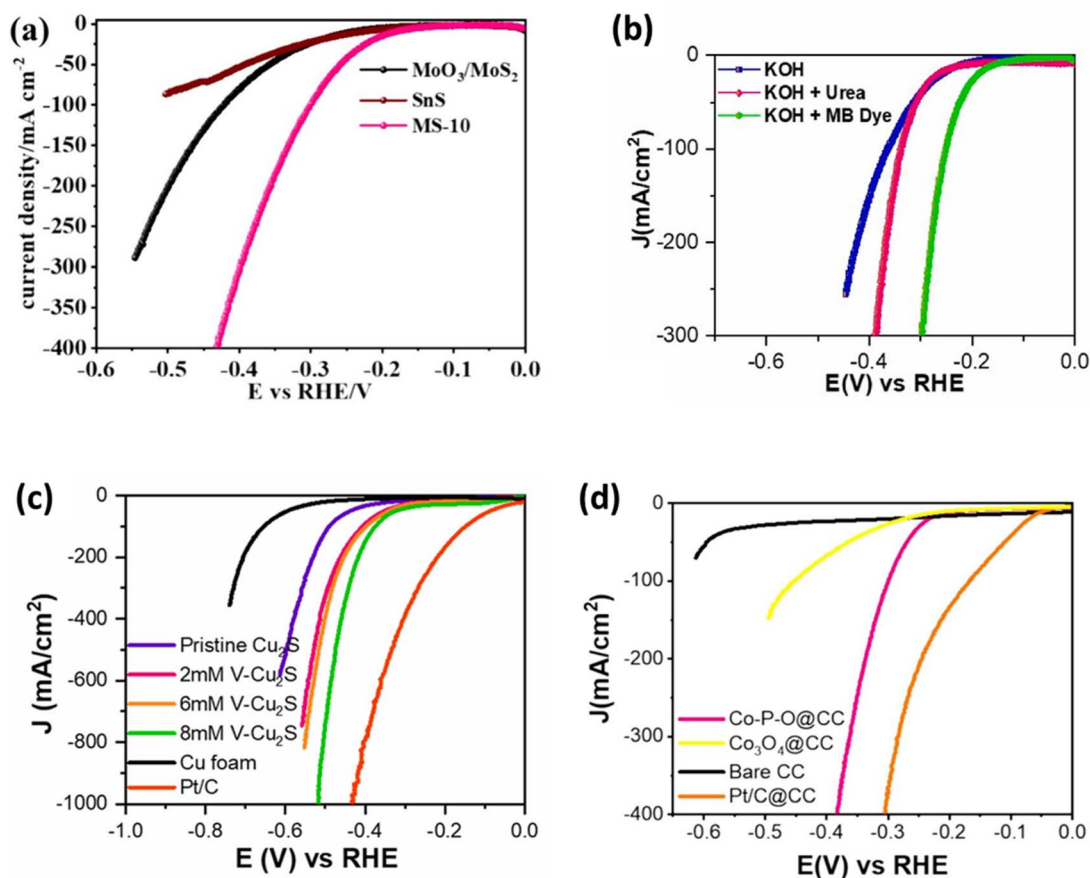


Fig. 6 Alkaline water electrolysis: (a) HER polarization curve of self-supported SnS/MoO<sub>3</sub> electrocatalyst. Reproduced with permission from ref. 64 copyright Journal of Energy Storage, 2024, (b) electrocatalytic HER activity of catalyst-embedded CuCo<sub>2</sub>S<sub>4</sub> electrode. Reproduced with permission from ref. 44 copyright International Journal of Hydrogen Energy, 2024, (c) HER polarization curve of self-supported V-Cu<sub>2</sub>S catalysts. Reproduced with permission from ref. 48 copyright International Journal of Hydrogen Energy, 2024, (d) polarization curves for HER performance on catalyst-embedded Co-P-O fabric. Reproduced with permission from ref. 65 copyright Journal of Electroanalytical Chemistry, 2024.



$\text{cm}^{-2}$  which is lower compared to that of  $\text{RuO}_2/\text{NF}||\text{Pt}/\text{C}/\text{NF}$  which is 1.9 V. Additionally, 100 h durability was tested at 1 A  $\text{cm}^{-2}$  owing to the excellent formation of heterojunctions that increases the electrocatalytic activity and can open doors for the industrial applications Fig. 5(e).<sup>59</sup>

Dhakal *et al.* formed the heterostructure by the *in situ* confined cobalt nanoparticles in nitrogen-doped carbon, which was derived from the zeolitic imidazolate framework-67, along with the composition of bimetallic cobalt vanadium phosphide, using a different technique. The  $\text{Co}_2\text{P-VP}@N\text{-C}/\text{Co}$  (+, -) was verified in an alkaline electrolyzer, which achieved low cell potentials of 1.49 V and 1.71 V at current densities of 10 and 100  $\text{mA cm}^{-2}$ , respectively. This is attributed to the modulation of the d-electronic configuration and the synergistic effect of the various heterointerfaces. The electrode demonstrated exceptional stability, operating continuously for 100 h at 100  $\text{mA cm}^{-2}$ . This work highlights the potential of metal foam-based catalyst-embedded electrodes as reproducible materials for green hydrogen production, offering a sustainable alternative for clean energy applications Fig. 5(f).<sup>60</sup> The detailed analysis of the catalysts in different electrolytes is presented in Table 3.

Modi *et al.* reported on the performance of a self-supported  $\text{SnS}/\text{MoO}_3$  electrocatalyst, which achieved a high current density of 400  $\text{mA cm}^{-2}$  at an overpotential of  $-0.43$  V vs. RHE.<sup>64</sup> This performance was attributed to the catalyst's unique porous structure with uniformly arranged nanosheets, as shown in Fig. 6(a). Joshi *et al.* presented the electrocatalytic HER activity of a  $\text{CuCo}_2\text{S}_4$  electrode, tested in KOH, KOH + urea, and KOH + methylene blue dye electrolytes, as depicted in Fig. 6(b). The high current density was attributed to the low oxidation potential of urea and organic dye, which facilitated rapid oxidation at the anode and accelerated hydrogen evolution at the cathode.<sup>44</sup> Sharma *et al.* studied the electrochemical performance of self-supported V- $\text{Cu}_2\text{S}$  nanoparticles on copper

foam using a three-electrode system in 1 M KOH, achieving a current density of 1000  $\text{mA cm}^{-2}$  Fig. 6(c). The enhanced HER activity was attributed to the V-doping strategy, which optimized the hydrogen-adsorption-free energy.<sup>48</sup> Additionally, Sharma *et al.* investigated the HER performance of Co-P-O fabric in 1.0 M KOH, reporting stability at high current densities ranging from 10 to 100  $\text{mA cm}^{-2}$ , as shown in Fig. 6(d). The rapid change in potential during cathodic current switching was linked to effective and stable electronic and mass transport, made possible by the self-supported nature of the electrode.<sup>65</sup>

Wu *et al.* presented a facile strategy for synthesizing a highly efficient HER catalyst composed of Pt single atoms (PtSA) anchored in Fe vacancies and Pt quantum dots (PtQD) on the surface of NiFe LDH. The catalyst demonstrated remarkable stability, withstanding 4000 CV cycles and 200 h of continuous hydrogen production. When used as the cathode in an alkaline water electrolyzer, it achieved exceptionally low cell voltages of 1.48 V and 1.73 V to reach current densities of 10 and 1000  $\text{mA cm}^{-2}$ , respectively.<sup>66</sup> Similar to Alkaline Water Electrolysis (AWE), Potassium Hydroxide (KOH) is frequently employed in Alkaline Exchange Membrane Water Electrolysis (AEMWE).<sup>57,67</sup> In contrast to conventional alkaline solutions, the alkaline exchange membrane is less tolerant of high pH, hence the electrolyte selection is crucial to ensuring compatibility.<sup>68,69</sup> Because of its advantageous ionic conductivity, KOH is a desirable option for the electrolyte because it must effectively conduct hydroxide ions ( $\text{OH}^-$ ).<sup>70,71</sup> To avoid degradation and preserve performance, the electrolyte and membrane must also get along. Thus, to guarantee membrane lifetime and overall system efficiency, the electrolyte's concentration and pH must be regulated (Fig. 7).<sup>70,72</sup>

Since sulfuric acid ( $\text{H}_2\text{SO}_4$ ) has high ionic conductivity and can be corrosive to some materials, it has been employed in proton exchange membrane water electrolysis (PEMWE).<sup>73,74</sup>

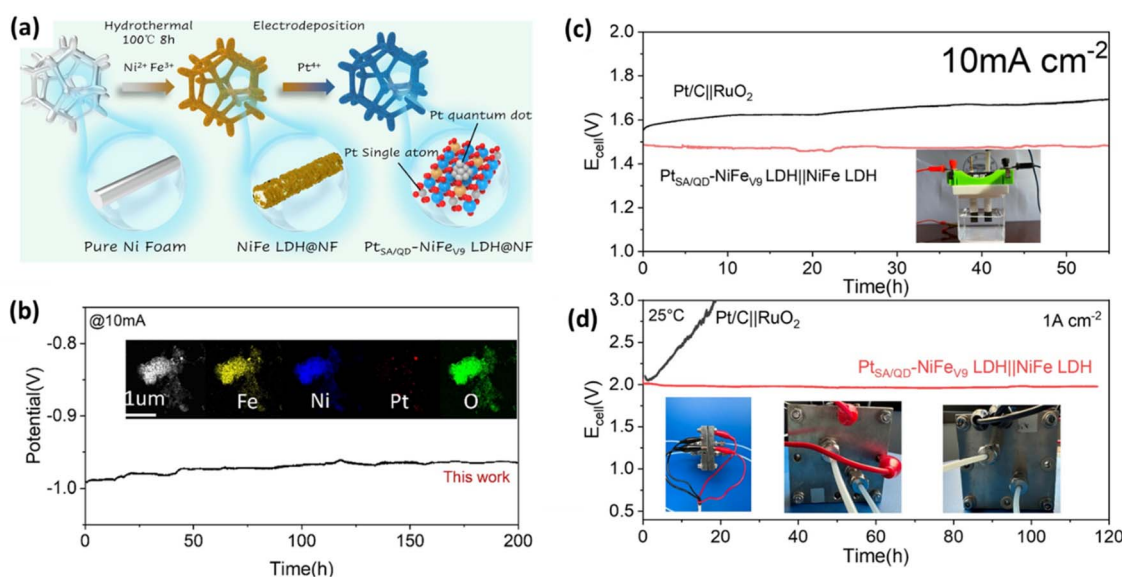


Fig. 7 High current density alkaline water electrolysis: (a) schematic illustration of the synthesis of Pt single atoms and quantum dots on NiFe LDH, (b) chronoamperometric analysis showing long-term stability, (c) long-term stability test for overall water splitting at 10  $\text{mA cm}^{-2}$ , (d) 1 A  $\text{cm}^{-2}$ . Reproduced with permission from ref. 66 copyright International Journal of Materials Science & Technology, 2025.



Phosphoric acid ( $\text{H}_3\text{PO}_4$ ) is also occasionally utilized. To guarantee excellent performance and efficiency, protons ( $\text{H}^+$ ) must be conducted efficiently by the electrolyte from the anode to the cathode.<sup>57,71,75</sup> To prevent deterioration or unfavorable reactions with the membrane and other components, it must also be chemically stable in acidic environments. Furthermore, to preserve membrane conductivity and performance in PEM systems, appropriate hydration management is necessary; the electrolyte should facilitate sufficient hydration without contributing to excessive swelling or membrane deterioration.<sup>56,71,76</sup> Since they are based on perfluorosulfonic acid (PFSA) polymers, proton exchange membranes (PEM) like Nafion are well-known for their superior proton conductivity and chemical stability in membrane design for electrolysis systems.<sup>77–79</sup> However, research is still being done to investigate alternative materials, such as hydrocarbon-based and composite membranes, to improve performance and reduce costs. High proton conductivity, chemical stability at high voltages and in acidic environments, and efficient water management to avoid dehydration or excessive swelling are important factors for PEMs.<sup>80,81</sup> Common varieties of Alkaline Exchange Membranes (AEM) based on quaternary ammonium polymers conduct hydroxide ions ( $\text{OH}^-$ ). These membranes must be able to effectively transport hydroxide ions, withstand high pH conditions, and have enough mechanical strength to withstand long-term operation.<sup>82</sup> Thicker membranes have lower resistance, but they must balance durability to prevent leaks or failure. Advanced designs, on the other hand, may combine composite or multi-layer topologies to improve conductivity and overall performance.

### 2.3 Effect on current density and voltage management: the use of binder and monomer

The performance of the electrolysis system is greatly impacted by the use of binders and monomers in the membrane and electrode materials, particularly current density and voltage control. In addition to distributing active components uniformly and maintaining high porosity for improved reactant access and gas release, binders—which offer structural integrity and guarantee good contact between active materials and current collectors—also aid in the achievement of high current densities.<sup>83</sup> As the building blocks of polymerization, monomers control the conductivity and structure of the polymer, which has an impact on ion transport and total current density. Regarding voltage control, monomers affect electrical resistance and chemical stability, which are essential for sustaining constant voltage performance, while binders help to mechanically stabilize and lower overpotential by guaranteeing enough electrical contact and heat dissipation.<sup>82</sup> To maximize ion transport, maintain structural integrity, and reduce resistive losses—all of which contribute to improved performance at high current densities and steady voltage operation—careful selection of binders and monomers is necessary.<sup>84</sup> Self-supported electrodes, which offer advantages in terms of both structure and performance, represent a breakthrough in electrolysis technology. These electrodes' inherent stability and

durability mean that they don't require extra support structures or current collectors, which simplifies system design and lowers material costs. Higher current densities and more effective mass transfer are made possible by their sophisticated materials and nanostructured or porous designs, which also increase active surface area and ionic conductivity. Additionally, this design decreases overpotential and resistive losses, hence lowering the additional voltage needed for electrochemical reactions.

Furthermore, self-supported electrodes help with efficient heat management, consistent voltage maintenance, and performance preservation. Constructed from conductive polymers, metal foams, or composites, these materials provide exceptional mechanical strength and conductivity.<sup>85</sup> However, for maximum longevity and performance, they must be compatible with particular membranes, such as PEM or AEM. Self-supported electrodes are a significant advancement in electrolysis technology since they enhance system performance, economy, and efficiency overall. Guan *et al.* reported the development of a multistage structural self-supported electrode through structural engineering on carbon nanofibers for efficient hydrogen evolution reaction at high current densities. The stable mechanical structure, along with the robust catalytic surface and electron donor design in the multi-level structure, provided exceptional stability. In a 100 h stability test at 100 mA  $\text{cm}^{-2}$ , the voltage variation was only 50 mV. Additionally, when the Pt@Co/CNFs self-supported electrode was used directly in an AEM water electrolysis system, a low cell voltage of 2.18 V was achieved at 500 mA  $\text{cm}^{-2}$ . As shown in Fig. 8, the electrode also demonstrated outstanding operational stability for over 200 h without significant performance degradation.<sup>83</sup> Park *et al.* reported the synthesis of self-supported Co–Ni–Cu–Mn electrocatalysts on porous carbon paper. This electrocatalyst was applied as a highly efficient cathode gas diffusion electrode for proton exchange membrane water electrolyzers (PEMWE). The PEMWE single cell, equipped with a Pt-free cathode, demonstrated excellent performance, achieving 2.57 A  $\text{cm}^{-2}$  at a cell voltage of 2.0 V, with exceptional stability maintained for 60 h at a high current density of 2.0 A  $\text{cm}^{-2}$ .<sup>84</sup> Therefore, the performance of water electrolysis systems is greatly improved by the use of self-supported electrodes, particularly when binders and monomers are applied strategically. When self-supported electrodes, like those made of multi-metal alloys (like Co–Ni–Cu–Mn), are used, supplementary conductive elements are not required, which lowers interfacial resistance and improves electron transport. High current densities are dependent on effective mass transfer, which is made possible by the catalyst's direct integration with the electrode substrate, which also maximizes the exposure of active sites.

### 2.4 Gas management and separation at high current density operation

The rate of evolution of hydrogen and oxygen gases increases dramatically at high current densities, causing gas bubbles to develop on the electrode surface. A process known as bubble masking occurs when these bubbles stick to the surface



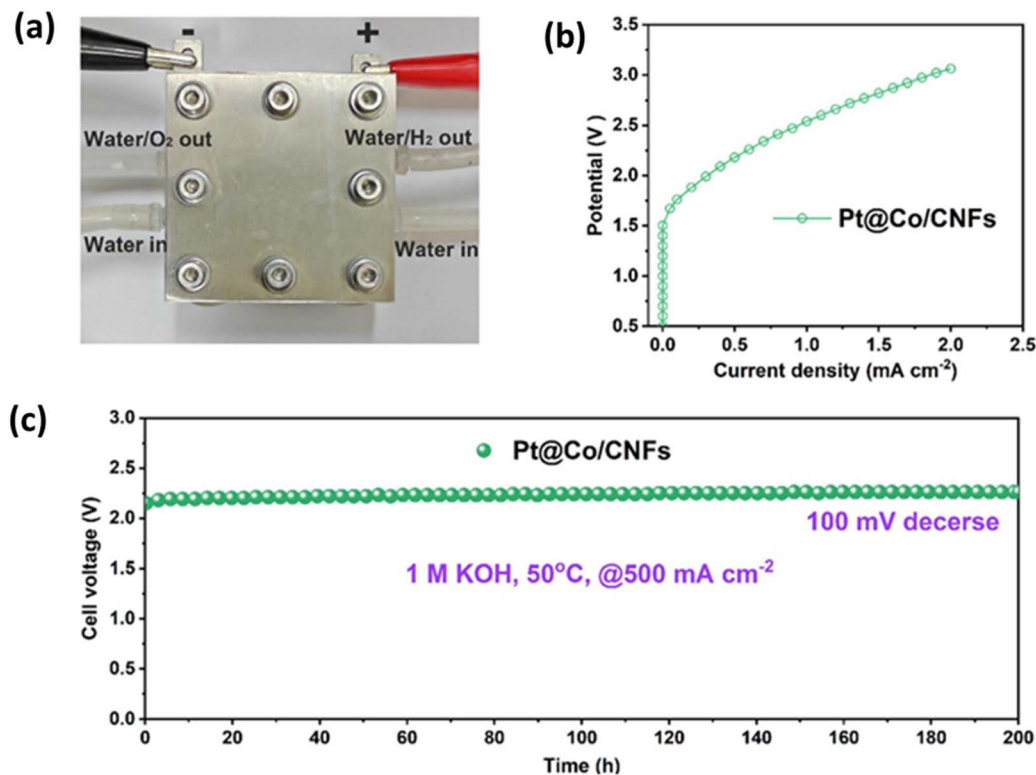


Fig. 8 (a) The AEM electrolyzer setup using self-supported Pt@Co/CNFs electrode, (b) polarization curves of the AEM electrolyzer measured at 50 °C in KOH, (c) electrochemical stability measurement of the electrode showing durability of the electrode. Reproduced with permission from ref. 83. Copyright Separation and Purification Technology, 2024.

preventing access to active areas and decreasing the effective area for electrochemical reactions.<sup>86,87</sup> The structural properties of nanostructured and porous electrodes enhance gas release, providing a solution to this problem. The pores and nano-features serve as pathways that let gas bubbles leave easily, keeping big bubbles from building up and guaranteeing that the active sites are always exposed to the electrolyte. Furthermore, hydrophobic characteristics can be incorporated into nanostructured surfaces to facilitate the quick detachment of gas bubbles and preserve a high active surface area even during aggressive gas production.<sup>88–90</sup> Additionally, because of their higher surface-to-volume ratio, these surfaces promote the development of smaller gas bubbles, which are simpler to separate and diffuse more quickly.<sup>87,91,92</sup> A flow-through configuration further enhances gas management in some porous electrode designs, including foams or meshes, by allowing gas bubbles to be transported away by the electrolyte flow, lowering the possibility of gas build-up and enabling prolonged high current density operation.<sup>15,49</sup> The effects of gas development at high current densities in zero-gap alkaline water electrolyzers were studied quantitatively by Deng *et al.* The electrolysis process's efficiency is greatly impacted by gas evolution, especially when current density is high. The principal methods by which gas bubbles result in reduced efficiency are the screening and voidage effects, which both interfere with the current and ion transport distribution, as further detailed in Fig. 9. When bubbles stick to the electrode surface, the

electrolyte gets displaced and localized current density spikes are produced. This is known as the screening effect. In the meantime, bubbles disrupt ion channels, increasing ohmic resistance and causing the voidage effect. Careful electrode and electrolyte design is essential to reduce these impacts and improve the efficiency and sustainability of electrolysis systems. Electrolysis efficiency can be increased by controlling gas bubble formation and optimizing electrode designs, particularly in high-demand applications such as hydrogen production.<sup>91</sup>

Sharma *et al.* conducted a dynamic-specific resistance test at a current density of 300 mA cm<sup>-2</sup> to investigate the behavior of gas bubble evolution and superhydrophobicity on self-supported nickel foam electrodes Fig. 10(a). The study highlighted the role of the nickel foam's 3D structure in improving gas management and sustaining efficient hydrogen production under high current densities. The study observed that sudden increases in specific resistance were attributed to the nucleation of hydrogen gas bubbles and their accumulation on the electrode surface, while sudden decreases in resistance corresponded to the expulsion of these bubbles.<sup>56</sup> The findings demonstrated that foam-based 3D electrodes can significantly enhance hydrogen production at high current densities without negatively impacting bubble evolution Fig. 10(b) and (c). This method allowed for analyzing bubble behavior on the electrode surface during electrolysis, offering insights into how gas bubble nucleation, build-up, and expulsion affect the



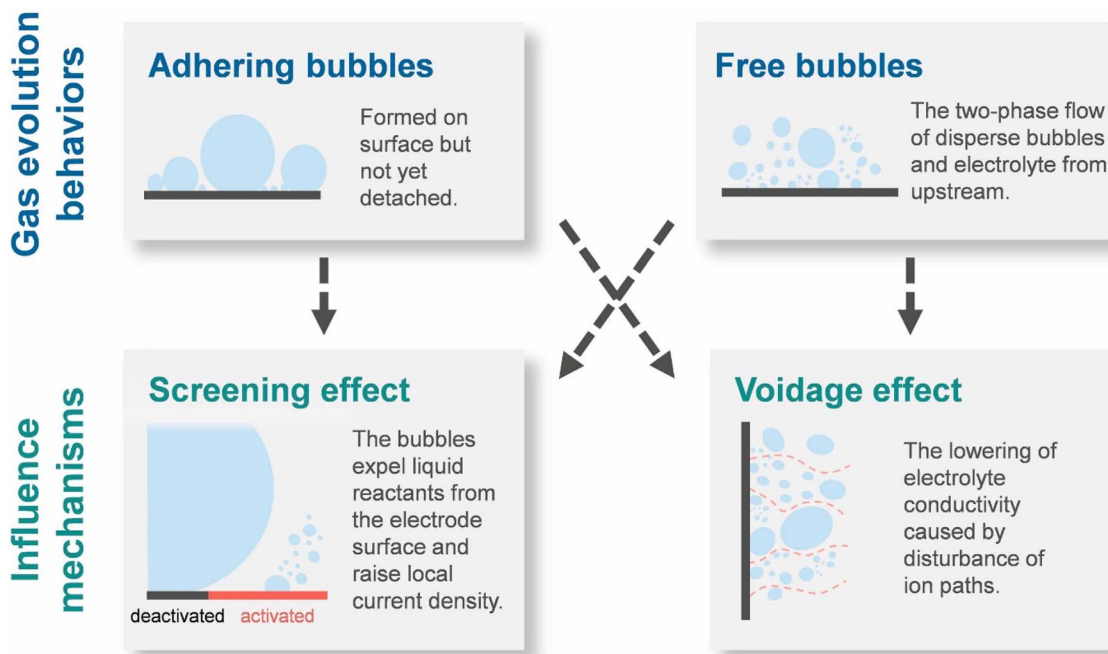


Fig. 9 Quantitative insights on gas evolution impact at high current densities. Reproduced with permission from ref. 91 copyright Journal of Power Sources, 2023.

electrode's performance. Thus, by using self-supported 3D network electrodes, the problems caused by gas evolution during electrolysis, specifically the screening and voidage effects, can be successfully reduced.<sup>56</sup> These advanced electrode configurations provide notable benefits in resolving the problems of bubble adhesion and ion route interference.<sup>43,56,65</sup> Better gas bubble management is made possible by the greater surface area and increased number of open channels that 3D network electrodes offer over traditional flat electrodes.<sup>93</sup> Gas bubbles quickly detach from the linked porous structure, lessening their adherence to the electrode surface and the screening effect. The increased surface area also aids in more uniformly dispersing the local current density, preventing current density spikes that, in the absence of the Tafel equation's prediction, would raise the electrolytic voltage.<sup>56,91</sup>

## 2.5 Optimizing cell stack design for efficient scale-up in commercial electrolyzers

The design of the cell stack in commercial electrolyzers plays a critical role in increasing hydrogen production while preserving dependability and efficiency. To maximize output, many electrolysis cells are stacked together; nevertheless, maintaining consistent performance across all cells depends on optimizing the stack design.<sup>94</sup> Effective flow control is crucial because it avoids localized fluctuations in current density, temperature, and performance, which can cause inefficiencies and uneven wear. Instead, water or electrolyte is distributed uniformly throughout the stack.<sup>95</sup> Vinodh *et al.* reviewed recent advancements in catalyst-coated membranes for water electrolysis, intended for use in various types of water electrolyzers. The study emphasized that the synergy between membrane

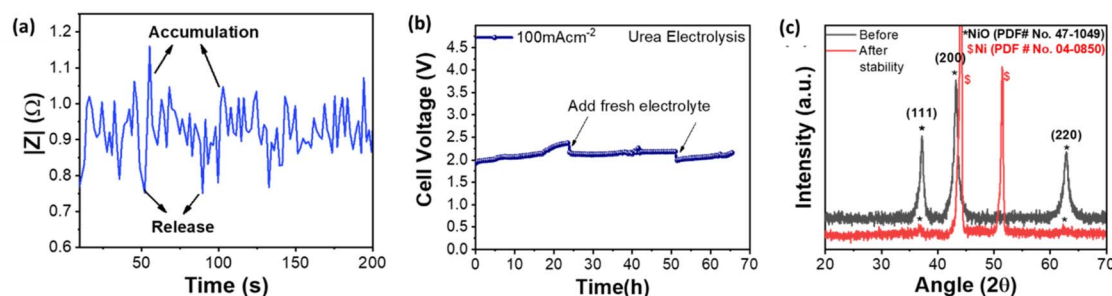


Fig. 10 (a) Dynamic-specific resistance test was performed to examine the evolution of gas bubbles and superhydrophobicity on self-supported nickel foam electrodes. (b) Stability measurement at high current density. (c) Structural stability of the self-supported nickel foam electrodes after 70 h of high current density operation and H<sub>2</sub> evolution. Reproduced with permission from ref. 56 copyright International Journal of Hydrogen Energy, 2024.



materials, catalyst layers, and supporting structures was crucial, highlighting the need for an integrated approach to refine membranes for improved electrochemical performance and extended operational longevity.<sup>96</sup> Phillips *et al.* presented a study on minimizing the ohmic resistance of an alkaline electrolysis cell through effective cell design. The effect of electrode morphology on the cell's ohmic resistance was demonstrated. The investigation examined how gas evolution influenced the ohmic resistance of the alkaline electrolysis cell. The reduction in ohmic resistance resulting from the use of a zero-gap design was quantified. Alkaline electrolysis at high current densities was shown to achieve both high efficiency and low cost.<sup>92</sup>

Furthermore, controlling the current distribution lowers the possibility of performance loss by guaranteeing that every cell functions at optimal levels. Effective heat dissipation is crucial for the stack to prevent overheating, which can deteriorate materials and decrease efficiency.<sup>94,97</sup> Another important consideration is mechanical integrity, since the cell stack needs to be strong enough to endure high temperatures, high pressures, and the strains of continuous operation without breaking down.<sup>97,98,99</sup> A sturdy, well-thought-out cell stack is necessary for the consistent, scalable production of hydrogen in commercial electrolyzers.

## 2.6 Enhancing operational stability for commercialization at high current densities

Commercializing water electrolysis systems requires improving their operational stability at high current densities since larger output rates put a lot of strain on the system's components. Dissipating the heat produced by resistive losses, which can deteriorate materials, dry membranes, and lower overall efficiency, requires effective thermal management.<sup>100,101</sup> Heat-dissipating materials, optimum cell stack designs, and sophisticated cooling systems contribute to temperature management that keeps performance from declining. Another important consideration is electrode endurance; materials must be able to resist strong electrochemical reactions without degrading. Long-term performance is ensured by self-supported, nanostructured, and porous electrodes, which give increased mechanical strength and resistance. Furthermore, gas bubble formation might obstruct active sites and reduce efficiency at high current densities. Key obstacles to the commercialization of water electrolyzers were outlined by Grigoriev, including the requirement for global integration, harmonization, unification, and standardization of components made by different suppliers. AI-driven automation and robots have the potential to significantly lower costs and accelerate large-scale implementation in the PEM water electrolyzer production process. Sustained innovation and extensive industrial expertise are essential for developing PEM electrolyzers of the next generation. Furthermore, policies, investments, subsidies, and assistance from the legislature all significantly contribute to the PEM water electrolyzer market's rapid expansion.<sup>102</sup> Gas masking is lessened by the use of nanostructured and porous electrodes, which enable effective gas escape and encourage the creation of

smaller bubbles. Improving the surface architecture of self-supported electrodes is one way to improve bubble release during electrolysis. This can be accomplished by building nanoarrays, which reduce the contact area between gas bubbles and the electrode, or by increasing surface porosity and roughness. Faster bubble detachment is made possible by these changes, which enhance mass transfer and catalytic efficiency overall.<sup>101,103</sup> Since alkaline exchange membranes (AEMs) and proton exchange membranes (PEMs) need to withstand chemical and mechanical deterioration while retaining ionic conductivity, proper membrane stability is also essential.<sup>101</sup> Improved water management membranes save you from drying out and maintain conductivity for extended high-density operations. Uniform water or electrolyte flow across the stack is essential for system integration and design, as inefficient flow distribution can result in localized differences in current density and lower system efficiency.<sup>101</sup> To provide a theoretical model for analyzing energy efficiency and forecasting physical and chemical changes under complex operating settings, Chen *et al.* looked into the heat and mass transport characteristics of PEMWE. Their research can inform performance forecasting and large-scale applications by providing insightful information on how to optimize PEMWE's structure and operating circumstances. This model establishes the theoretical groundwork for further developments in PEMWE, especially when it comes to attaining high current density in practical uses.<sup>104</sup> Optimizing the porous transport layer (PTL) is necessary to achieve efficient polymer electrolyte membrane water electrolysis (PEMWE) with low noble metal-free-loaded electrolyzers. The PTL is important but has not received enough attention, particularly concerning its impact on overpotentials. Investigating the effects of PTL porosity, thickness, and structure on PEMWE performance, Hasa *et al.* discovered that adding a microporous layer enhances the PTL-catalyst layer contact, improving electron transfer and oxygen removal. This tactic lowers cell voltage and increases efficiency, and it is especially effective at low catalyst loadings.<sup>105</sup> Bi *et al.* used experimental data to validate their voltage model as they examined the voltage characteristics of an alkaline electrolyzer at various temperatures, pressures, and current densities. The findings demonstrated that raising the temperature and current density increased system efficiency and decreased energy consumption, however, there were ideal values for each parameter. Efficiency was most closely correlated with current density, and performance was improved at greater temperatures, although equipment and financial constraints had to be taken into account. Pressure fluctuations had little impact on system efficiency and energy consumption, showing limited advantages from pressure adjustments.<sup>106</sup> Long-term operation at high pressures and temperatures depends on the mechanical integrity of the electrolyzer stack, necessitating the use of materials that can resist these conditions without deforming or failing.<sup>105,107</sup> Since catalysts must withstand structural alterations or degradation, which can happen at high current densities, catalytic stability is equally crucial. The creation of long-lasting catalysts is essential to lowering overpotentials and guaranteeing sustained effectiveness.<sup>108</sup> Water electrolysis systems can be optimized to produce



hydrogen on a large scale with dependability by taking into account the following factors: thermal management, gas bubble accumulation, membrane durability, system integration, and catalyst stability. This will make the systems sustainable and commercially viable for the future.<sup>106</sup> In hydrogen generation, the integration of self-supported electrodes is essential to achieving key performance indicators (KPIs). These electrodes make production processes more standardized and straightforward, which promotes industrialization and scale-up. Self-supported designs increase overall system efficiency by reducing the amount of electrical energy needed to produce one unit of hydrogen through increased catalytic efficiency. Furthermore, self-supported electrodes' resilience increases the electrolyzers' operating lifespan, which lowers expenses by spreading the initial investment across a higher amount of hydrogen production and improving the technology's economic viability.

### 3 Advances in water electrolysis for industrial-scale hydrogen production

As was mentioned, scaling up for high current densities, high temperatures, and fluctuating pressures necessary for large-scale hydrogen production poses several difficulties for water electrolysis systems working under industrially relevant circumstances.<sup>97,109</sup> By addressing these problems, recent research has significantly improved the effectiveness, robustness, and commercial viability of electrolysis systems. In commercial electrolysis, reaching high current densities ( $\geq 1 \text{ A cm}^{-2}$ ) is crucial because it optimizes the production of hydrogen.<sup>81,94</sup> To reduce overpotentials and enhance mass transport, however, sustained performance at these high densities necessitates optimizing both the catalyst and electrode designs. PGMs and non-precious metal oxides are examples of advanced nanostructured catalysts that have demonstrated increased activity and durability; self-supported electrodes, on the other hand, are better able to withstand the mechanical and thermal stresses that these catalysts must withstand.<sup>110</sup> More effective gas evolution is made possible by nanostructured and porous electrode materials, such as carbon-based supports and nickel foam, which also improve gas bubble release and lower mass transport constraints.<sup>111</sup> Another important consideration is thermal control because industrial electrolyzers produce a lot of heat, which, if left unchecked, can result in overheating, membrane drying, and decreased system efficiency. Both passive and active cooling methods, such as liquid-cooled cell stacks and heat-resistant materials that aid in evenly dispersing heat throughout the stack, have been studied recently. It has been demonstrated that operating at high pressure and temperature improves hydrogen purity and improves reaction kinetics, but it also puts stress on sealing mechanisms and membranes.<sup>106</sup> Cutting-edge membrane materials have proven to have improved thermal and chemical stability, retaining mechanical integrity and ionic conductivity in industrial settings.<sup>112</sup> Long-term performance depends on membrane hydration, and materials that efficiently control

water transport have been created through research to avoid dehydration and provide operational stability at high current densities.<sup>113</sup> Because prolonged high-current operations can cause catalyst sintering, corrosion, or surface deterioration, catalyst stability continues to be a major concern.<sup>114</sup> High-entropy alloys (HEAs) and transition metal-based alloys, which resist degradation and retain high activity in harsh environments, are examples of durable catalysts that have been the subject of study to address this. Additionally, self-healing catalysts that renew while in use have come to light as a potential way to increase the lifespan of catalysts.<sup>113,115</sup> Finally, optimizing stack design to manage rising current and production demands is necessary for expanding electrolysis systems to industrial capacity.<sup>116</sup> To improve mass transport and heat dissipation, computational fluid dynamics (CFD) models have been used to design more effective flow fields.<sup>95,117,118</sup> Meanwhile, advances in mechanical stack design, such as modular configurations and resilient seals, guarantee long-term operational integrity under high pressure and temperature.<sup>119</sup> All of these developments are opening the door for the commercialization of water electrolysis devices that can reliably and efficiently create hydrogen on an industrial scale.<sup>120</sup>

#### 3.1 Benchmarking protocols for industrial-scale green hydrogen production

To advance green hydrogen production by water electrolysis at industrial scales, state-of-the-art catalyst development and appropriate benchmarking techniques are necessary. Recent research has produced major advancements in catalyst innovation with an emphasis on lowering overpotentials and increasing the effectiveness of hydrogen and oxygen evolution processes (HER and OER).<sup>121–123</sup> Advances in nanostructured catalysts, like high-entropy alloys (HEAs)<sup>124</sup> and transition metal oxides,<sup>125</sup> have shown to be very successful, providing greater mass transport, bigger surface areas, and long-term stability in challenging industrial settings. Particularly noteworthy is HEAs' ability to withstand sintering and corrosion, which makes them perfect for long-term high-current density operations.<sup>126</sup> Gas diffusion, active charge transport, stability, and durability were all improved by self-supported electrodes that made use of strong 3D nickel foam or carbon scaffolds, which also increased durability and efficiency.<sup>119,127</sup> Furthermore, system designs are becoming simpler, and total prices are decreasing due to bifunctional catalysts that can drive both HER and OER. Additionally, innovative materials that show promise are performing better at high current densities.<sup>128</sup> To supplement these developments, thorough benchmarking techniques were created to evaluate the viability of catalysts in practical applications. Advanced techniques such as cyclic voltammetry (CV), electrochemical impedance spectroscopy (EIS), and linear sweep voltammetry (LSV) are utilized to evaluate key metrics, such as durability, turnover frequency (TOF), and overpotential.<sup>129</sup> These techniques offer valuable insights into reaction kinetics, mass transport, and long-term stability under a range of industrial conditions.<sup>91,130–132</sup> These developments in catalyst design and standardized benchmarking are driving the



development of green hydrogen generation systems for industrial use. For electrolysis systems to produce green hydrogen that is scalable, dependable, and efficient, they must meet benchmarking requirements.<sup>128,133–135</sup>

*In situ* electrochemical measurements, including X-ray photoelectron spectroscopy (XPS), Fourier-transform infrared spectroscopy (FTIR), and Raman spectroscopy, have been significantly integrated into these protocols in recent research, improving our understanding of catalyst performance, material stability, and reaction dynamics.<sup>88,136</sup> For example, real-time monitoring of the vibrational modes of molecules on the catalyst surface during electrolysis can be achieved through Raman spectroscopy.<sup>131</sup> This real-time monitoring provides insights

into the oxidation states and reaction intermediates involved in the oxygen evolution reaction (OER) and hydrogen evolution reaction (HER).<sup>137,138</sup> Comparably, FTIR spectroscopy provides insightful information on the surface chemistry and functional groups of catalysts while they are in use, clarifying the kinetics and reaction processes that are essential for comparing catalyst performance, efficiency, and scalability.<sup>131,139,140</sup>

As depicted in Fig. 11, Chen *et al.* presented an illustration of the *in situ* cell configurations for differential electrochemical mass spectrometry (DEMS), *in situ* Raman spectroelectrochemistry, *in situ* UV-vis Spectro electrochemistry, and *in situ* attenuated total reflectance infrared (ATR-IR) spectroelectrochemistry.<sup>138</sup> These configurations are employed in typical

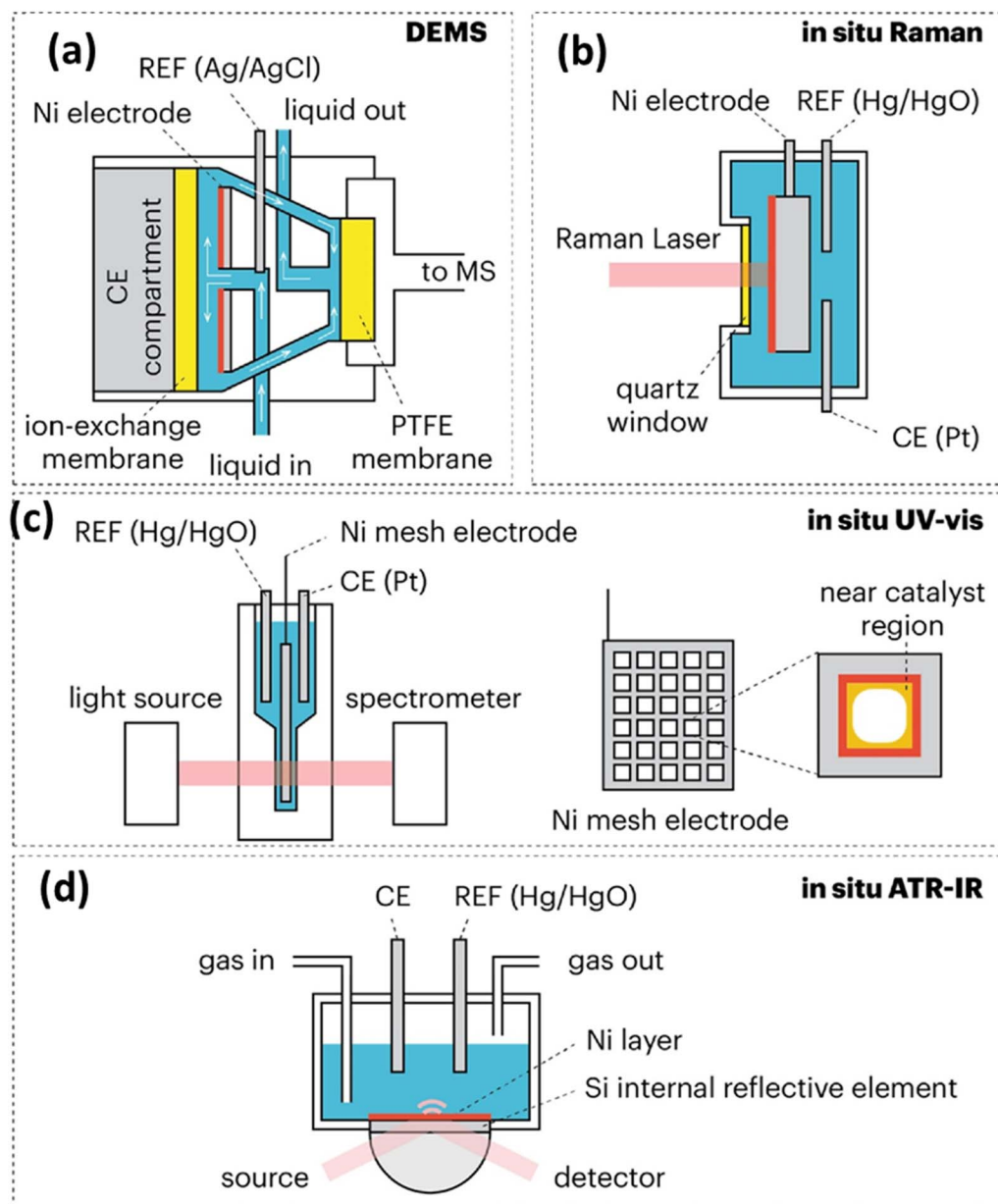


Fig. 11 Illustration of selected *in situ* cell configurations. (a) Differential electrochemical mass spectrometry (DEMS); (b) *in situ* Raman Spectro electrochemistry; (c) *in situ* UV-vis Spectro electrochemistry; (d) *in situ* attenuated total reflectance infrared (ATR-IR) Spectro electrochemistry. Reproduced with permission from ref. 138. Copyright Journal of Catalysis, 2024.



electrochemical reactions, offering valuable insights into promising pathways for environmental remediation, energy conversion, and the production of value-added chemicals. When it comes to examining the surface composition and chemical states of catalysts both before and after electrolysis, XPS is a priceless tool for identifying variations in surface species and oxidation states that affect catalytic activity and stability.<sup>141,142</sup> An effective method for comprehending the electrical and local structure of electrocatalysts during operational conditions is X-ray spectroscopy. Non-electroactive substances are also essential to electrocatalytic processes, even though electroactive species are what initiate the catalysis process. The efficiency of these reactions is strongly influenced by cations, anions, solvents, and reactants. Mendoza *et al.* examined the current status of *in situ/operando* X-ray spectroscopy experiments focused on electroactive species in their discussion of the electrochemical reduction of carbon dioxide. They also offered insights into methods and configurations that could be used to study non-electroactive species.<sup>142</sup> Zhu *et al.* conducted an *in situ* Raman study on intermediate adsorption engineering through high-index facet control during the hydrogen evolution reaction.<sup>143</sup> The representative results, shown in Fig. 12, highlight emerging trends in measurements aimed at understanding material stability. These findings are

crucial for evaluating the suitability of materials for commercial-scale hydrogen production and assessing the long-term stability of electrodes.

Recent research has shown how successful these methods are, showing how they may offer a thorough comprehension of molecular structural alterations and their impact on overall cell function. According to studies, for instance, *in situ* measurements make it easier to evaluate long-term stability since they show how catalysts change over extended periods of operational stress, which is essential for creating durability benchmarks.<sup>144</sup> This comprehensive method helps to build efficient, long-lasting, and affordable hydrogen production systems in addition to helping to optimize operational variables, including temperature, pressure, and current density.<sup>145</sup> The incorporation of these sophisticated characterization methods into benchmarking protocols is consistent with the scientific community's continuous endeavours to facilitate the shift to sustainable energy sources, which in turn propels progress in the generation of green hydrogen.<sup>143,146</sup>

### 3.2 Best practices for high current density operation in water electrolysis systems

Recent developments in water electrolysis systems highlight the necessity for best practices to handle the enormous mechanical

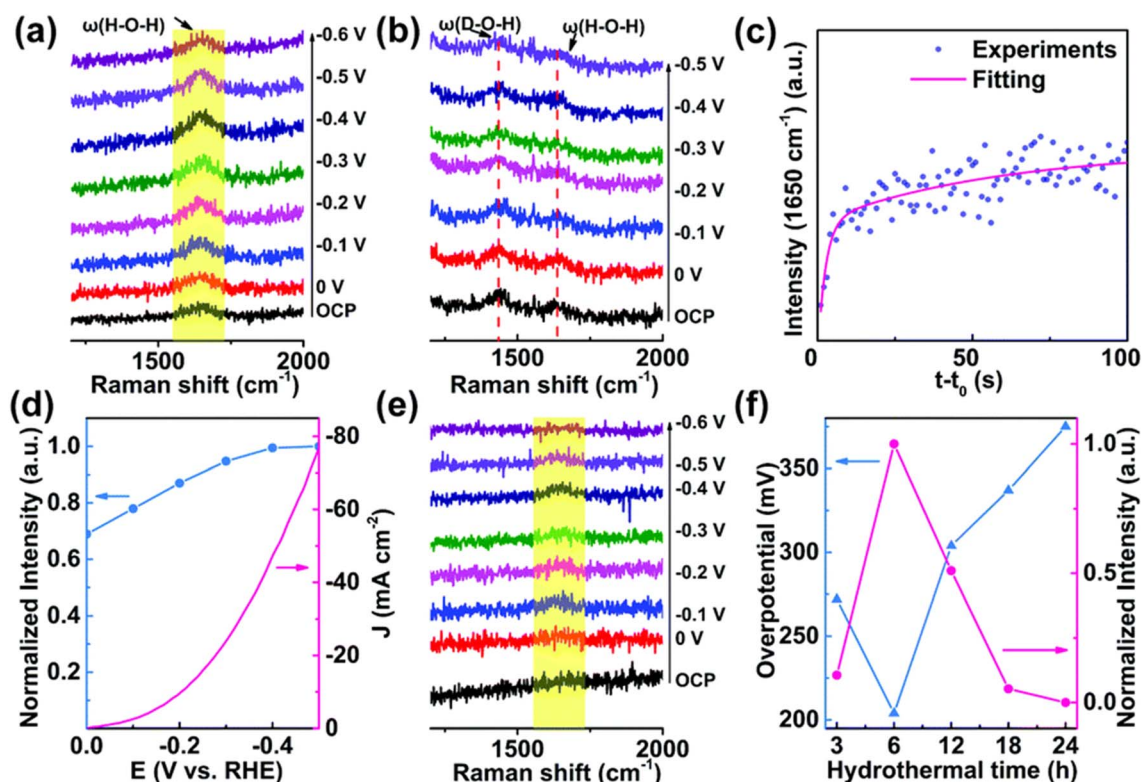
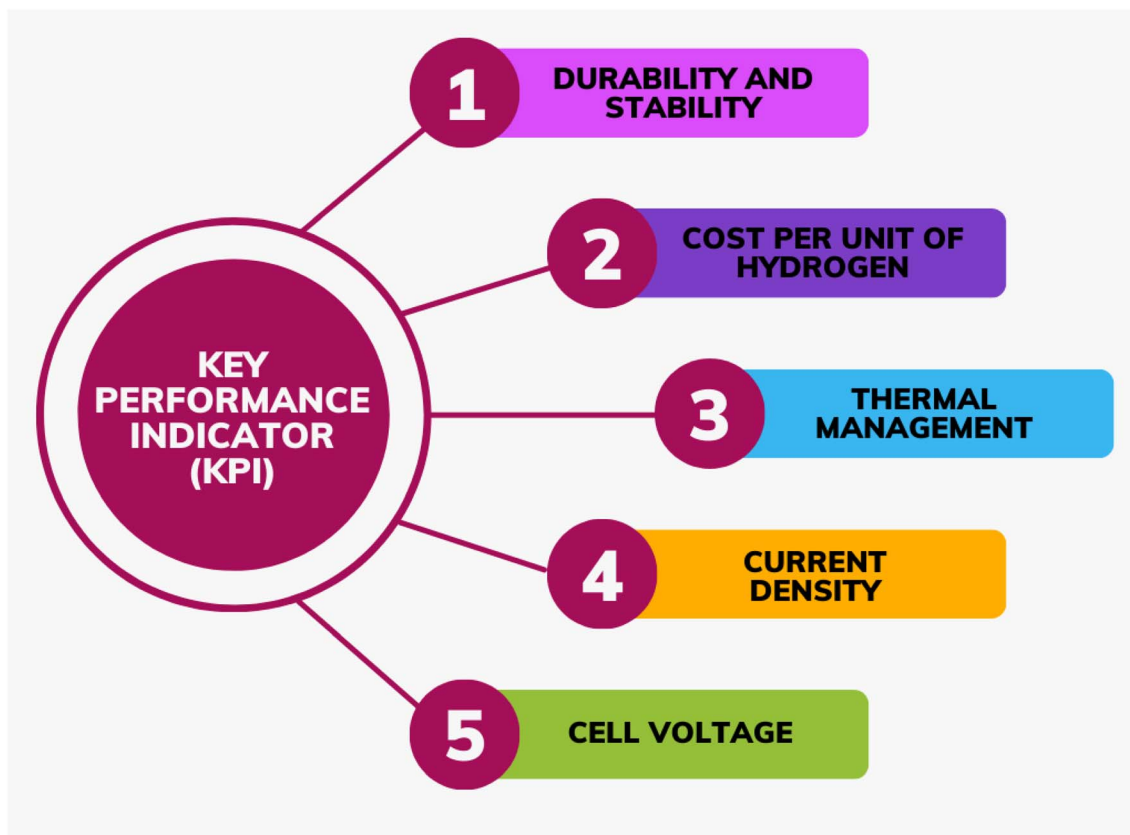


Fig. 12 *In situ* Raman spectra of Ti@TiO<sub>2</sub>-6H nanosheets recorded from 0 V to -0.6 V vs. RHE in different solutions: (a) 1 M KOH and (b) 0.5 M KOH + 0.5 M KOD. (c) Time-dependent intensity of the Raman peak at 1650 cm<sup>-1</sup> on Ti@TiO<sub>2</sub>-6H nanosheets at -0.5 V vs. RHE. (d) Normalized intensity of the Raman peak at ~1650 cm<sup>-1</sup> on the surface of Ti@TiO<sub>2</sub>-6H nanosheets, along with the corresponding LSV curves from 0 V to -0.9 V vs. RHE, scanned at 10 mV s<sup>-1</sup>. (e) *In situ* Raman spectra of Ti@TiO<sub>2</sub>-18H nanosheets from 0 V to -0.6 V vs. RHE. (f) Normalized intensity of the Raman peak at ~1650 cm<sup>-1</sup> at -0.5 V vs. RHE, and overpotentials at 10 mA cm<sup>-2</sup> on Ti@TiO<sub>2</sub> nanosheets with varying hydrothermal times. All experiments were conducted in 1.0 M KOH solution, except for isotope labeling experiments. Reproduced with permission from ref. 143. Copyright Inorganic Chemistry Frontiers, 2020.





Scheme 3 Key Performance Indicators (KPIs).

and thermal loads on system components, especially for those running at high current densities ( $\geq 1 \text{ A cm}^{-2}$ ).<sup>146</sup> Efficient thermal management is essential to avoid problems like membrane dehydration and catalyst degradation. Newer developments in this area include integrated cooling technologies that ensure uniform temperature distribution and reduce localized hotspots by integrating cooling channels into the electrode and membrane structures.<sup>147</sup> Industrial-scale operations with significant heat loads are also successful with hybrid cooling systems that include liquid and air cooling. Simultaneously, advances in electrode and catalyst design have led to the development of nanostructured and porous electrodes.<sup>9</sup> Examples of these electrodes include those composed of graphene-based materials or 3D nickel foam, which improve efficiency by reducing bubble build-up and enhancing gas diffusion.<sup>148</sup> Stronger than ever, self-supported electrodes with built-in catalysts provide longevity and mechanical strength without requiring additional supports.<sup>147,148</sup> Computational fluid dynamics (CFD) simulations optimize flow-field designs to ensure equal electrolyte distribution and minimize pressure differentials, ensuring stable operation. Effective flow management is another crucial component.<sup>95,100,136,149</sup> Improvements in resistance to deterioration and hydration maintenance have resulted from advances in membrane technology, particularly composite proton exchange membranes (PEMs) and alkaline exchange membranes (AEMs), which are essential for preserving performance at high current densities. Additionally,

by evaluating operational data to anticipate possible problems like membrane dehydration or catalyst deactivation, machine learning (ML) is being used more and more to improve system performance and predictive maintenance.<sup>150,151</sup> These best practices are essential for scaling up water electrolysis systems for industrial green hydrogen production, as they ensure both efficiency and cost-effectiveness in large-scale applications.<sup>57,127,151</sup> They are driven by state-of-the-art research in thermal management, electrode and catalyst design, flow distribution, membrane stability, and predictive maintenance.<sup>81,121</sup>

## 4 Conclusion and future outlook

The review briefly elaborates the key parameters for the production of green hydrogen at high current density. The design of electrolyzers that can outperform at an industrial scale requires the detailed study of electrocatalysts, the effect of highly alkaline-acidic electrolytes, and optimizations of the results. The number of electrodes is reported for that performance at higher current density ( $>1000 \text{ mA cm}^{-2}$ ). However, the electrodes are well-justified in lab-scale surroundings, but the employment of the catalyst at a commercial scale requires evaluation in similar harsh conditions. In this review, we have summarised the role of self-supported electrodes and their study in various electrolytes. The review consists of vivid 3D supports that can sustain in highly alkaline and seawater



conditions. Moreover, the bifunctional study of these catalyst materials and their durability (>100 h) at high current density (>500 mA cm<sup>-2</sup>) has been briefly mentioned in this review.

To push up hydrogen production at higher current densities, some important parameters should be optimized. Scheme 3 prioritized key performance indicators (KPIs) to provide better insight into electrolyzers' assessment. The durability of the electrolyzers plays a vital role in enhancing their lifespan. The commercial-scale hydrogen production requires >1000 mA cm<sup>-2</sup> to survive for approximately >100 h.<sup>152</sup> Additionally, the aggressive environment, such as highly acidic-alkaline electrolytes, extreme temperatures, and immense evolution of gases, blocks the productivity of the industrial-scale electrolyzer. The tailoring of the mechanical stability of the material during the detachment of the gas molecules can enable the electrode to withstand the high current density.<sup>153</sup> The generation of green hydrogen from the ocean has attracted direct electrolysis on a commercial scale. However, the seawater is home to highly concentrated chlorine anion (Cl<sup>-</sup>), which, on oxidation, degrades the anodic electrode, resulting in faster corrosion and a decrease in its efficiency. Therefore, the self-supported NiCoP foam was synthesized over nickel foam using the dynamic hydrogen bubble template technique (DHBT). The work significantly focuses on producing green hydrogen from the alkaline seawater. The electrocatalyst displayed recognizably low overpotentials of about 328 mV and 356 mV for the HER and OER mechanisms, respectively, to achieve the large current density of 1000 mA cm<sup>-2</sup>. This is due to the formation of oxyhydroxy group and PO<sub>4</sub><sup>3+</sup>, which provides more active sites and reduces the effect of Cl<sup>-</sup> ions. Additionally, the work has outperformed reported catalysts by surviving for over 300 h in alkaline seawater at 1000 mA cm<sup>-2</sup>.<sup>154</sup> Green hydrogen production in the US using water electrolyzers is roughly \$4 per kg which is estimated to be reduced to \$2.16 per kg by the year 2030. The US government aims to reduce production costs by \$1 per kg. The optimization of various barriers, like the development of self-supported non-noble electrocatalysts with equivalent efficiency. As per the Oxford Institute of Energy Studies, the electrolysis system makes up 15% of the total cost share in the hydrogen generation system.

Lowering the cost of its components, like the membrane in the PEM electrolyzers, can drastically reduce the cost per unit.<sup>155,156</sup> Thermal control plays a critical role in preserving the efficiency and stability of the system, avoiding overheating, and guaranteeing smooth operation at high current densities. The channels for coolant along the setups can rapidly cool down the system's heat. Apart from this, designing the electrolyzers that can be adjusted with the heat generation can successfully encourage industrial applications. Electrode material capable of sustaining at high temperatures can not only produce hydrogen faster without compromising its efficiency. Maintaining a high current density (e.g., 500–1000 mA cm<sup>-2</sup>) without sacrificing efficiency is critical for scaling up production.<sup>150,157</sup> The increase in current density directly increases the number of reactions occurring on the interstitial sites of the electrodes. These reactions are responsible for the damage to the electrode in the long term. Therefore, a detailed analysis and the

performance of the electrode should be optimised before anchoring as excellent electrocatalysts.<sup>158</sup> The current density is directly linked to the cell voltage of the electrolyzer. The amount of hydrogen produced is controlled by the current density, while the amount of power utilized is controlled by both the cell voltage and current. Currently, the electrolyzers require high cell voltage to achieve the desired current density, which hinders the efficiency of the system. The increase in cell voltage is associated with the higher electrolyte resistance due to the temperature rise. Therefore, the solution to the increased temperature and medium resistance can lower the cell voltage. This is connected to the longer life cycle of the electrode. Furthermore, maintaining low cell voltages (e.g., 1.48 V for 10 mA cm<sup>-2</sup> and 1.73 V for 1000 mA cm<sup>-2</sup>) guarantees that operations remain energy-efficient even when subjected to heavy loads.<sup>159,160</sup>

Keeping the key parameters and the criteria for the development of robust 3D electrocatalyst which can withstand the harsh conditions and could perform outstanding results for industrial purposes can open the idea of utilizing hydrogen driven technology in place of fossil fuels can be achieved in near future.

## Data availability

No primary research results, software or code have been included and no new data were generated or analysed as part of this review.

## Conflicts of interest

The authors declare that they have no known competing financial interests or personal relationships that could have appeared to influence the work reported in this paper.

## Acknowledgements

The authors are grateful to the DST-Inspire fellowship (IF190690) and the Gujarat State Biotechnology Mission (GSBTM/JD/(R&D)/662/2022–23/00292122) for the financial support. The CHARUSAT University is acknowledged by the authors for providing research facilities.

## References

- Z. Li, *et al.*, Transition metal-based self-supported anode for electrocatalytic water splitting at a large current density, *Coord. Chem. Rev.*, 2023, **495**, 215381, DOI: [10.1016/j.ccr.2023.215381](https://doi.org/10.1016/j.ccr.2023.215381).
- J. Liang, *et al.*, Aqueous alternating electrolysis prolongs electrode lifespans under harsh operation conditions, *Nat. Commun.*, 2024, **15**(1), 6208, DOI: [10.1038/s41467-024-50519-2](https://doi.org/10.1038/s41467-024-50519-2).
- Q. Zhou, L. Liao, H. Zhou, D. Li, D. Tang and F. Yu, Innovative strategies in design of transition metal-based catalysts for large-current-density alkaline water/seawater



- electrolysis, *Mater. Today Phys.*, 2022, **26**, 100727, DOI: [10.1016/j.mtphys.2022.100727](https://doi.org/10.1016/j.mtphys.2022.100727).
- 4 J. Liang, *et al.*, Electroreduction of alkaline/natural seawater: self-cleaning Pt/carbon cathode and on-site co-synthesis of H<sub>2</sub> and Mg hydroxide nanoflakes, *Chem*, 2024, **10**(10), 3067–3087, DOI: [10.1016/j.chempr.2024.05.018](https://doi.org/10.1016/j.chempr.2024.05.018).
  - 5 T. Wu, *et al.*, Recent advances and strategies of electrocatalysts for large current density industrial hydrogen evolution reaction, *Inorg. Chem. Front.*, 2023, **10**(16), 4632–4649, DOI: [10.1039/D3Q100799E](https://doi.org/10.1039/D3Q100799E).
  - 6 Y. Wan, L. Zhou and R. Lv, Rational design of efficient electrocatalysts for hydrogen production by water electrolysis at high current density, *Mater. Chem. Front.*, 2023, **7**(23), 6035–6060, DOI: [10.1039/D3QM00722G](https://doi.org/10.1039/D3QM00722G).
  - 7 S. Chen, *et al.*, Advances of layered double hydroxide electrocatalysts for high-current-density alkaline water/seawater splitting, *Coord. Chem. Rev.*, 2024, **510**, 215832, DOI: [10.1016/j.ccr.2024.215832](https://doi.org/10.1016/j.ccr.2024.215832).
  - 8 Z. Zou, K. Dastafkan, Y. Shao, C. Zhao and Q. Wang, Electrocatalysts for alkaline water electrolysis at ampere-level current densities: a review, *Int. J. Hydrogen Energy*, 2024, **51**, 667–684, DOI: [10.1016/j.ijhydene.2023.07.026](https://doi.org/10.1016/j.ijhydene.2023.07.026).
  - 9 S. V. Chauhan, K. K. Joshi, P. M. Pataniya and C. K. Sumesh, *Catalyst-Anchored 3D Framework Electrodes: A Breakthrough in Large-Scale Hydrogen Production*, John Wiley and Sons Inc, 2025, DOI: [10.1002/ppsc.202400226](https://doi.org/10.1002/ppsc.202400226).
  - 10 F. Y. Chen, Z. Y. Wu, Z. Adler, and H. Wang, *Stability challenges of electrocatalytic oxygen evolution reaction: From mechanistic understanding to reactor design*, Cell Press, 2021, vol. 21, DOI: [10.1016/j.joule.2021.05.005](https://doi.org/10.1016/j.joule.2021.05.005).
  - 11 Q. Xu, *et al.*, Anion Exchange Membrane Water Electrolyzer: Electrode Design, Lab-Scaled Testing System and Performance Evaluation, *EnergyChem*, 2022, **4**(5), 100087, DOI: [10.1016/j.enchem.2022.100087](https://doi.org/10.1016/j.enchem.2022.100087).
  - 12 H. Sun, X. Xu, H. Kim, W. C. Jung, W. Zhou and Z. Shao, *Electrochemical Water Splitting: Bridging the Gaps between Fundamental Research and Industrial Applications*, 2023, DOI: [10.1002/eem2.12441](https://doi.org/10.1002/eem2.12441).
  - 13 T. Y. Ma, S. Dai and S. Z. Qiao, Self-supported electrocatalysts for advanced energy conversion processes, *Mater. Today*, 2016, **19**(5), 265–273, DOI: [10.1016/j.mattod.2015.10.012](https://doi.org/10.1016/j.mattod.2015.10.012).
  - 14 X. Zhang, *et al.*, Noble-Metal-Free Oxygen Evolution Reaction Electrocatalysts Working at High Current Densities over 1000 mA cm<sup>-2</sup>: From Fundamental Understanding to Design Principles, *Energy Environ. Mater.*, 2023, **6**(5), e12457, DOI: [10.1002/eem2.12457](https://doi.org/10.1002/eem2.12457).
  - 15 P. J. Sharma, K. H. Modi, P. Sahatiya, C. K. Sumesh and P. M. Pataniya, Electroless deposited NiP-fabric electrodes for efficient water and urea electrolysis for hydrogen production at industrial scale, *Appl. Surf. Sci.*, 2024, **644**, 158766, DOI: [10.1016/j.apsusc.2023.158766](https://doi.org/10.1016/j.apsusc.2023.158766).
  - 16 P. Chauhan, D. J. Late, V. Patel, P. Sahatiya and C. K. Sumesh, Hierarchical NiCo-LDH@MoS<sub>2</sub>/CuS composite as efficient trifunctional electrocatalyst for overall water splitting and asymmetric supercapacitor, *Electrochim. Acta*, 2023, **469**, 143197, DOI: [10.1016/j.electacta.2023.143197](https://doi.org/10.1016/j.electacta.2023.143197).
  - 17 S. V. Chauhan, K. K. Joshi, P. M. Pataniya, P. Sahatiya, G. Bhadu and C. K. Sumesh, Fe<sub>2</sub>B/MXene@NF electrocatalyst for efficient water splitting and green hydrogen production at high current densities, *Renew. Energy*, 2025, **241**, 122370, DOI: [10.1016/j.renene.2025.122370](https://doi.org/10.1016/j.renene.2025.122370).
  - 18 D. Shao, *et al.*, A designed hierarchical porous Cu–Ni/Ni–Cu alloy converted from commercial nickel foam as versatile electrocatalysts for efficient and extremely stable water splitting, *J. Colloid Interface Sci.*, 2025, 137565, DOI: [10.1016/j.jcis.2025.137565](https://doi.org/10.1016/j.jcis.2025.137565).
  - 19 S. Khatun, S. Pal and P. Roy, Surface oxygen vacancy engineering of Cr-doped FeNi<sub>3</sub>/NiFe<sub>2</sub>O<sub>4</sub> Mott-Schottky heterojunction as efficient electrocatalyst for high current density water oxidation, *J. Alloys Compd.*, 2024, **977**(September 2023), 173393, DOI: [10.1016/j.jallcom.2023.173393](https://doi.org/10.1016/j.jallcom.2023.173393).
  - 20 S. Paygozar, A. Sabour Rouhaghdam, A. Seif and G. Barati Darband, *In situ* electrochemical synthesis of superhydrophilic NiCoMn trimetallic-alloy nanosheets via the dynamic hydrogen bubble template method for developing high current density hydrogen production electrocatalysts, *J. Mater. Chem. A*, 2024, **12**(40), 27558–27569, DOI: [10.1039/D4TA03698K](https://doi.org/10.1039/D4TA03698K).
  - 21 K. K. Joshi, P. M. Pataniya, G. Bhadu, P. Sahatiya and C. K. Sumesh, Defect-engineered tri-metallic CuCoSnOx heterostructure bifunctional electrocatalysts for energy-efficient hydrogen production at high current density, *Int. J. Hydrogen Energy*, 2024, **96**, 46–58, DOI: [10.1016/j.ijhydene.2024.11.325](https://doi.org/10.1016/j.ijhydene.2024.11.325).
  - 22 S. A. Dristy, S. Lin, M. A. Habib, M. H. Joni, R. Mandavkar and J. Lee, Manganese doped NiBP: a promising electrocatalyst for sustainable hydrogen production at high-current-density (HCD), *Int. J. Hydrogen Energy*, 2024, **96**, 321–332, DOI: [10.1016/j.ijhydene.2024.11.283](https://doi.org/10.1016/j.ijhydene.2024.11.283).
  - 23 C. Sun, C. Wang, G. Han, Y. Zhang and H. Zhao, Pt atomic clusters/MoS<sub>2</sub> nanosheets/Co-doped hollow carbon nanofibers for high-current-density alkaline hydrogen production, *Chem. Eng. J.*, 2024, **496**, 153665, DOI: [10.1016/j.cej.2024.153665](https://doi.org/10.1016/j.cej.2024.153665).
  - 24 Q. Zhao, *et al.*, In-situ growth of ZIF-67-derived Co/wood-based carbon self-supporting electrocatalysts for stable hydrogen evolution at high current density, *Int. J. Hydrogen Energy*, 2024, **96**, 235–243, DOI: [10.1016/j.ijhydene.2024.11.247](https://doi.org/10.1016/j.ijhydene.2024.11.247).
  - 25 R. Ren, Y. Wang and T. Li, In situ growth of FeCo sulfides on cobalt iron foam for efficient high-current-density hydrogen evolution reaction electrocatalysis, *J. Colloid Interface Sci.*, 2025, **682**, 288–297, DOI: [10.1016/j.jcis.2024.11.251](https://doi.org/10.1016/j.jcis.2024.11.251).
  - 26 X. Mu, *et al.*, Robust water/seawater-electrolysis hydrogen production at industrial-scale current densities by modulating built-in-outer electric field of catalytic substance, *Nano Energy*, 2024, **131**, 110216, DOI: [10.1016/j.nanoen.2024.110216](https://doi.org/10.1016/j.nanoen.2024.110216).



- 27 N. Hussain, *et al.*, A tricomponent low-cost composite material comprising bimetallic Cu-Ni nanoparticles anchored on 2D layered MoS<sub>2</sub> as an electrocatalyst for hydrogen production through seawater splitting, *J. Power Sources*, 2025, **630**, 236180, DOI: [10.1016/j.jpowsour.2025.236180](https://doi.org/10.1016/j.jpowsour.2025.236180).
- 28 D. Li, *et al.*, High current density hydrogen evolution on heterostructured Ni/Cr bimetallic sulfide catalyst in alkaline media, *Int. J. Hydrogen Energy*, 2024, **49**, 67–74, DOI: [10.1016/j.ijhydene.2023.06.299](https://doi.org/10.1016/j.ijhydene.2023.06.299).
- 29 Y. Luo, *et al.*, Stabilized hydroxide-mediated nickel-based electrocatalysts for high-current-density hydrogen evolution in alkaline media, *Energy Environ. Sci.*, 2021, **14**(8), 4610–4619, DOI: [10.1039/D1EE01487K](https://doi.org/10.1039/D1EE01487K).
- 30 Z. Chen, *et al.*, Hierarchical porous NiFe-P@NC as an efficient electrocatalyst for alkaline hydrogen production and seawater electrolysis at high current density, *Inorg. Chem. Front.*, 2023, **10**(5), 1493–1500, DOI: [10.1039/D2QI02703H](https://doi.org/10.1039/D2QI02703H).
- 31 Y. Chen, *et al.*, Metallic Ni<sub>3</sub>Mo<sub>3</sub>N Porous Microrods with Abundant Catalytic Sites as Efficient Electrocatalyst for Large Current Density and Superstability of Hydrogen Evolution Reaction and Water Splitting, *Appl. Catal., B*, 2020, **272**, 118956, DOI: [10.1016/j.apcatb.2020.118956](https://doi.org/10.1016/j.apcatb.2020.118956).
- 32 T. Wang, X. Cao and L. Jiao, Ni<sub>2</sub>P/NiMoP heterostructure as a bifunctional electrocatalyst for energy-saving hydrogen production, *eScience*, 2021, **1**(1), 69–74, DOI: [10.1016/j.esci.2021.09.002](https://doi.org/10.1016/j.esci.2021.09.002).
- 33 Y. Tang, *et al.*, Multifunctional carbon-armored Ni electrocatalyst for hydrogen evolution under high current density in alkaline electrolyte solution, *Appl. Catal., B*, 2023, **321**, 122081, DOI: [10.1016/j.apcatb.2022.122081](https://doi.org/10.1016/j.apcatb.2022.122081).
- 34 X. Zhai, *et al.*, Accelerated dehydrogenation kinetics through Ru, Fe dual-doped Ni<sub>2</sub>P as bifunctional electrocatalyst for hydrazine-assisted self-powered hydrogen generation, *Nano Energy*, 2023, **105**, 108008, DOI: [10.1016/j.nanoen.2022.108008](https://doi.org/10.1016/j.nanoen.2022.108008).
- 35 Z. Ni, C. Luo, B. Cheng, P. Kuang, Y. Li and J. Yu, Construction of hierarchical and self-supported NiFe-Pt<sub>3</sub>Ir electrode for hydrogen production with industrial current density, *Appl. Catal., B*, 2023, **321**, 122072, DOI: [10.1016/j.apcatb.2022.122072](https://doi.org/10.1016/j.apcatb.2022.122072).
- 36 S. Lin, *et al.*, Fabrication of Ru-doped CuMnBP micro cluster electrocatalyst with high efficiency and stability for electrochemical water splitting application at the industrial-level current density, *J. Colloid Interface Sci.*, 2025, **677**, 587–598, DOI: [10.1016/j.jcis.2024.08.009](https://doi.org/10.1016/j.jcis.2024.08.009).
- 37 Y. Wu, *et al.*, Ultrastable NiFeOOH/NiFe/Ni electrocatalysts prepared by in-situ electro-oxidation for oxygen evolution reaction at large current density, *Appl. Surf. Sci.*, 2021, **564**, 150440, DOI: [10.1016/j.apsusc.2021.150440](https://doi.org/10.1016/j.apsusc.2021.150440).
- 38 D. Senthil Raja, C.-L. Huang, Y.-A. Chen, Y. Choi and S.-Y. Lu, Composition-balanced trimetallic MOFs as ultra-efficient electrocatalysts for oxygen evolution reaction at high current densities, *Appl. Catal., B*, 2020, **279**, 119375, DOI: [10.1016/j.apcatb.2020.119375](https://doi.org/10.1016/j.apcatb.2020.119375).
- 39 Y. Luo, *et al.*, Morphology and surface chemistry engineering toward pH-universal catalysts for hydrogen evolution at high current density, *Nat. Commun.*, 2019, **10**(1), 269, DOI: [10.1038/s41467-018-07792-9](https://doi.org/10.1038/s41467-018-07792-9).
- 40 P. Wang, *et al.*, MnO<sub>x</sub>-Decorated Nickel-Iron Phosphides Nanosheets: Interface Modifications for Robust Overall Water Splitting at Ultra-High Current Densities, *Small*, 2022, **18**(7), 2105803, DOI: [10.1002/smll.202105803](https://doi.org/10.1002/smll.202105803).
- 41 W. He, *et al.*, Super-Hydrophilic Microporous Ni(OH)<sub>x</sub>/Ni<sub>3</sub>S<sub>2</sub> Heterostructure Electrocatalyst for Large-Current-Density Hydrogen Evolution, *Small*, 2023, **19**(2), 2205719, DOI: [10.1002/smll.202205719](https://doi.org/10.1002/smll.202205719).
- 42 X.-Y. Zhang, *et al.*, Hydrogen evolution under large-current-density based on fluorine-doped cobalt-iron phosphides, *Chem. Eng. J.*, 2020, **399**, 125831, DOI: [10.1016/j.cej.2020.125831](https://doi.org/10.1016/j.cej.2020.125831).
- 43 H. K. Thakkar, *et al.*, Vertically Oriented FeNiO Nanosheet Array for Urea and Water Electrolysis at Industrial-Scale Current Density, *ACS Sustain. Chem. Eng.*, 2024, **12**(22), 8340–8352, DOI: [10.1021/acssuschemeng.4c00591](https://doi.org/10.1021/acssuschemeng.4c00591).
- 44 K. K. Joshi, S. V. Chauhan, P. M. Pataniya and C. K. Sumesh, Efficient hybrid water splitting and direct electrooxidation of organic dye from wastewater using copper cobalt sulphide nanosheets, *Int. J. Hydrogen Energy*, 2024, **58**, 1562–1575, DOI: [10.1016/j.ijhydene.2024.01.330](https://doi.org/10.1016/j.ijhydene.2024.01.330).
- 45 K. K. Joshi, P. M. Pataniya, G. R. Bhadu and C. K. Sumesh, Cu<sub>2</sub>CoSnS<sub>4</sub> electrocatalyst embedded paper working electrodes for efficient, stable, pH universal, and large-current-density hydrogen evolution reaction, *Int. J. Hydrogen Energy*, 2024, **49**, 829–842, DOI: [10.1016/j.ijhydene.2023.09.185](https://doi.org/10.1016/j.ijhydene.2023.09.185).
- 46 H. Wang, *et al.*, Tungstate Intercalated NiFe Layered Double Hydroxide Enables Long-Term Alkaline Seawater Oxidation, *Small*, 2024, **20**(28), 2311431, DOI: [10.1002/smll.202311431](https://doi.org/10.1002/smll.202311431).
- 47 A. M. Shah, *et al.*, Self-Supported Mn-Ni<sub>3</sub>Se<sub>2</sub> Electrocatalysts for Water and Urea Electrolysis for Energy-Saving Hydrogen Production, *ACS Appl. Mater. Interfaces*, 2024, **16**(9), 11440–11452, DOI: [10.1021/ACSAMI.3C16244/SUPPL\\_FILE/AM3C16244\\_SI\\_001.PDF](https://doi.org/10.1021/ACSAMI.3C16244/SUPPL_FILE/AM3C16244_SI_001.PDF).
- 48 P. J. Sharma, *et al.*, Self-supported V-Cu<sub>2</sub>S catalysts for green hydrogen production through alkaline water electrolysis, *Int. J. Hydrogen Energy*, 2024, **84**, 97–105, DOI: [10.1016/j.ijhydene.2024.08.224](https://doi.org/10.1016/j.ijhydene.2024.08.224).
- 49 N. Trivedi, *et al.*, Self-supported Cr-Cu<sub>2</sub>S nanoflakes for hydrogen production from seawater, *Int. J. Hydrogen Energy*, 2024, **49**, 1113–1122, DOI: [10.1016/j.ijhydene.2023.11.036](https://doi.org/10.1016/j.ijhydene.2023.11.036).
- 50 M. L. Frederiksen, M. V. Kragh-Schwarz, A. Bentien, L. P. Nielsen and P. Lu, Performance of Co-Co(OH)<sub>2</sub> coated nickel foam as catalysts for the hydrogen evolution reaction under industrially relevant conditions, *Int. J. Hydrogen Energy*, 2024, **49**, 668–675, DOI: [10.1016/j.ijhydene.2023.08.367](https://doi.org/10.1016/j.ijhydene.2023.08.367).
- 51 Y. Gui, *et al.*, One-step electrodeposition synthesis of NiFePS on carbon cloth as self-supported electrodes for



- electrochemical overall water splitting, *J. Colloid Interface Sci.*, 2024, **673**, 444–452, DOI: [10.1016/j.jcis.2024.06.096](https://doi.org/10.1016/j.jcis.2024.06.096).
- 52 Y. Liu, *et al.*, In Situ Engineering Multifunctional Active Sites of Ruthenium–Nickel Alloys for pH-Universal Ampere-Level Current-Density Hydrogen Evolution, *Small*, 2024, **20**(34), 2311509, DOI: [10.1002/SMLL.202311509](https://doi.org/10.1002/SMLL.202311509).
- 53 W. Zheng, M. Liu and L. Y. S. Lee, Best Practices in Using Foam-Type Electrodes for Electrocatalytic Performance Benchmark, *ACS Energy Lett.*, 2020, **5**(10), 3260–3264, DOI: [10.1021/ACSENERGYLETT.0C01958/ASSET/IMAGES/LARGE/NZ0C01958\\_0004.JPEG](https://doi.org/10.1021/ACSENERGYLETT.0C01958/ASSET/IMAGES/LARGE/NZ0C01958_0004.JPEG).
- 54 Y. Kuang, S. Zhao, S. Gao and N. Song, CoNi-phosphides with iron incorporation effectively boost hydrogen evolution reaction and oxygen evolution reaction for overall water splitting, *Int. J. Hydrogen Energy*, 2024, **83**, 1184–1192, DOI: [10.1016/j.ijhydene.2024.08.208](https://doi.org/10.1016/j.ijhydene.2024.08.208).
- 55 D. Mo, *et al.*, Co-doped NiSe synthesized on solid-phase boronized self-supported NFF-B as a bifunctional electrocatalyst enables efficient and stable overall water splitting, *Appl. Surf. Sci.*, 2024, **669**, 160452, DOI: [10.1016/j.apsusc.2024.160452](https://doi.org/10.1016/j.apsusc.2024.160452).
- 56 P. J. Sharma, *et al.*, Enhanced water and urea electrolysis at industrial scale current density using self-supported VxNi1-xO trifunctional catalysts, *Int. J. Hydrogen Energy*, 2024, **85**, 374–384, DOI: [10.1016/j.ijhydene.2024.08.352](https://doi.org/10.1016/j.ijhydene.2024.08.352).
- 57 R. A. Marquez, *et al.*, A Guide to Electrocatalyst Stability Using Lab-Scale Alkaline Water Electrolyzers, *ACS Energy Lett.*, 2024, **9**(2), 547–555, DOI: [10.1021/ACSENERGYLETT.3C02758/SUPPL\\_FILE/NZ3C02758\\_SI\\_002.MP4](https://doi.org/10.1021/ACSENERGYLETT.3C02758/SUPPL_FILE/NZ3C02758_SI_002.MP4).
- 58 S. Rezaee, S. Shahrokhian and Q. Li, In-situ stabilization of metal-nitride sites in sprouted 2D cMOF@LDHs heteronano petals on metaloxynitrides nanostems for enhanced water splitting, *J. Colloid Interface Sci.*, 2024, **671**, 394–409, DOI: [10.1016/j.jcis.2024.05.180](https://doi.org/10.1016/j.jcis.2024.05.180).
- 59 L. Liu, *et al.*, The cobalt-based metal organic frameworks array derived CoFeNi-layered double hydroxides anode and CoP/FeNi2P heterojunction cathode for ampere-level seawater overall splitting, *J. Colloid Interface Sci.*, 2024, **676**, 52–60, DOI: [10.1016/j.jcis.2024.07.098](https://doi.org/10.1016/j.jcis.2024.07.098).
- 60 P. P. Dhakal, *et al.*, Cobalt nanoparticles confined nitrogen-doped carbon integrated bimetallic Co2P–VP heterostructured composite: a MOF integrated 3D arrays for catalytic water splitting, *Compos. B Eng.*, 2024, **283**, 111640, DOI: [10.1016/j.compositesb.2024.111640](https://doi.org/10.1016/j.compositesb.2024.111640).
- 61 M. Yue, *et al.*, Co-doped Ni3S2 nanosheet array: a high-efficiency electrocatalyst for alkaline seawater oxidation, *Nano Res.*, 2024, **17**(3), 1050–1055, DOI: [10.1007/s12274-023-6002-6](https://doi.org/10.1007/s12274-023-6002-6).
- 62 Q. Dai, *et al.*, Cauliflower-like Ni3S2 foam for ultrastable oxygen evolution electrocatalysis in alkaline seawater, *Nano Res.*, 2024, **17**(8), 6820–6825, DOI: [10.1007/s12274-024-6744-9](https://doi.org/10.1007/s12274-024-6744-9).
- 63 J. Liang, *et al.*, Efficient bubble/precipitate traffic enables stable seawater reduction electrocatalysis at industrial-level current densities, *Nat. Commun.*, 2024, **15**(1), 2950, DOI: [10.1038/s41467-024-47121-x](https://doi.org/10.1038/s41467-024-47121-x).
- 64 K. H. Modi, P. M. Pataniya, G. Bhadu and C. K. Sumesh, Self-supported SnS/MoO3 electrocatalyst for supercapacitor and hydrogen evolution reaction, *J. Energy Storage*, 2024, **99**, 113475, DOI: [10.1016/j.est.2024.113475](https://doi.org/10.1016/j.est.2024.113475).
- 65 P. J. Sharma, S. Siraj, P. Sahatiya, C. K. Sumesh and P. M. Pataniya, Electroless plating of CoPO electrocatalyst on carbon cloth for alkaline water electrolysis, *J. Electroanal. Chem.*, 2024, **967**, 118491, DOI: [10.1016/j.jelechem.2024.118491](https://doi.org/10.1016/j.jelechem.2024.118491).
- 66 Y. Wu, *et al.*, Modulating the synergy of Pt single atoms and quantum dots on NiFe LDH for efficient and robust hydrogen evolution, *J. Mater. Sci. Technol.*, 2025, **215**, 111–120, DOI: [10.1016/j.jmst.2024.07.025](https://doi.org/10.1016/j.jmst.2024.07.025).
- 67 Y. Li, *et al.*, In-situ construction and repair of high catalytic activity interface on corrosion-resistant high-entropy amorphous alloy electrode for hydrogen production in high-temperature dilute sulfuric acid electrolysis, *Chem. Eng. J.*, 2023, **453**(Feb), 139905, DOI: [10.1016/j.cej.2022.139905](https://doi.org/10.1016/j.cej.2022.139905).
- 68 Q. Xu *et al.*, Anion Exchange Membrane Water Electrolyzer: Electrode Design, Lab-Scaled Testing System and Performance Evaluation, Elsevier B.V., 2022, DOI: [10.1016/j.enchem.2022.100087](https://doi.org/10.1016/j.enchem.2022.100087).
- 69 M. Chatenet, *et al.*, Water electrolysis: from textbook knowledge to the latest scientific strategies and industrial developments, *Chem. Soc. Rev.*, 2022, **51**(11), 4583–4762, DOI: [10.1039/d0cs01079k](https://doi.org/10.1039/d0cs01079k).
- 70 M. Plevová, J. Hnát, and K. Bouzek, *Electrocatalysts for the oxygen evolution reaction in alkaline and neutral media. A comparative review*, Elsevier B.V., 2021, vol. 30, DOI: [10.1016/j.jpowsour.2021.230072](https://doi.org/10.1016/j.jpowsour.2021.230072).
- 71 G. Gao, *et al.*, Recent advances in hydrogen production coupled with alternative oxidation reactions, *Coord. Chem. Rev.*, 2024, **509**(March), 215777, DOI: [10.1016/j.ccr.2024.215777](https://doi.org/10.1016/j.ccr.2024.215777).
- 72 H. Yang, M. Driess and P. W. Menezes, *Self-Supported Electrocatalysts for Practical Water Electrolysis*, John Wiley and Sons Inc, 2021, DOI: [10.1002/aenm.202102074](https://doi.org/10.1002/aenm.202102074).
- 73 S. Xue, Y. Gao, B. Wang and L. Zhi, Effects of external physical fields on electrocatalysis, *Chem Catal.*, 2023, 100762, DOI: [10.1016/j.checat.2023.100762](https://doi.org/10.1016/j.checat.2023.100762).
- 74 Y. Zhang, *et al.*, Design of modified MOFs electrocatalysts for water splitting: high current density operation and long-term stability, *Appl. Catal., B*, 2023, **336**(May), 122891, DOI: [10.1016/j.apcatb.2023.122891](https://doi.org/10.1016/j.apcatb.2023.122891).
- 75 S. C. Jesudass, *et al.*, Defect engineered ternary metal spinel-type Ni-Fe-Co oxide as bifunctional electrocatalyst for overall electrochemical water splitting, *J. Colloid Interface Sci.*, 2024, **663**(January), 566–576, DOI: [10.1016/j.jcis.2024.02.042](https://doi.org/10.1016/j.jcis.2024.02.042).
- 76 P. P. Puthiyaveetil, A. Torris, S. Dilwale, F. Kanheerampockil and S. Kurungot, Cathode|Electrolyte Interface Engineering by a Hydrogel Polymer Electrolyte for a 3D Porous High-Voltage Cathode Material in a Quasi-Solid-State Zinc Metal Battery by In Situ Polymerization, *Small*, 2024, 2403158, DOI: [10.1002/SMLL.202403158](https://doi.org/10.1002/SMLL.202403158).



- 77 H. Liu, *et al.*, Highly recyclable and efficient piezocatalyst of Nafion decorated MoS<sub>2</sub> with hierarchical structure for organic pollutants degradation, *Sep. Purif. Technol.*, 2023, 320(May), 124142, DOI: [10.1016/j.seppur.2023.124142](https://doi.org/10.1016/j.seppur.2023.124142).
- 78 D. K. Sarfo, J. Crawford, J. D. Riches and A. P. O'Mullane, Confining the electrodeposition of FeCoNi oxide within a Nafion layer for the fabrication of stable oxygen evolution electrocatalysts, *Chem Catal.*, 2023, 100750, DOI: [10.1016/j.checat.2023.100750](https://doi.org/10.1016/j.checat.2023.100750).
- 79 J. Ge, *et al.*, Investigation of the electrocatalytic mechanisms of urea oxidation reaction on the surface of transition metal oxides, *J. Colloid Interface Sci.*, 2022, 620, 442, DOI: [10.1016/j.jcis.2022.03.152](https://doi.org/10.1016/j.jcis.2022.03.152).
- 80 B. Li, L. Dai, G. L. Su, Z. Xia, Y. Ye and Z. Li, Construction of defective MnCo-LDH nanoflowers with high activity for overall water splitting, *Fuel*, 2024, 364(January), 130961, DOI: [10.1016/j.fuel.2024.130961](https://doi.org/10.1016/j.fuel.2024.130961).
- 81 V. Mastronardi, *et al.*, Alkaline electrochemical deposition of Pt for alkaline electrolyzers, *Int. J. Hydrogen Energy*, 2024, 80, 261–269, DOI: [10.1016/j.ijhydene.2024.07.086](https://doi.org/10.1016/j.ijhydene.2024.07.086).
- 82 M. Cao, *et al.*, Rational Construction of a 3D Self-Supported Electrode Based on ZIF-67 and Amorphous NiCoP for an Enhanced Oxygen Evolution Reaction, *Inorg. Chem.*, 2024, 14062, DOI: [10.1021/acs.inorgchem.4c01863](https://doi.org/10.1021/acs.inorgchem.4c01863).
- 83 J. Guan, *et al.*, Multistage structural self-supported electrode via structural engineering on carbon nanofibers for efficient hydrogen evolution reaction at high current density, *Sep. Purif. Technol.*, 2024, 347, 127628, DOI: [10.1016/j.seppur.2024.127628](https://doi.org/10.1016/j.seppur.2024.127628).
- 84 Y. Park, *et al.*, Synergistic enhancement of surface-doped Mn and Cu-mediated hierarchical reconstruction in Co-Ni-Cu-Mn electrocatalyst for hydrogen production in proton exchange membrane water electrolyzer, *J. Alloys Compd.*, 2024, 993, 174649, DOI: [10.1016/j.jallcom.2024.174649](https://doi.org/10.1016/j.jallcom.2024.174649).
- 85 R. P. Patel, P. M. Pataniya, S. Siraj, P. Sahatiya and C. K. Sumesh, Simultaneous production of green hydrogen and decontamination of dye wastewater using WSe<sub>2</sub>-CuO/graphite electrochemical cell, *Int. J. Hydrogen Energy*, 2024, 55, 815–827, DOI: [10.1016/j.ijhydene.2023.11.246](https://doi.org/10.1016/j.ijhydene.2023.11.246).
- 86 Y. Liu, X. Lu, Y. Peng and Q. Chen, Electrochemical Visualization of Gas Bubbles on Superaerophobic Electrodes Using Scanning Electrochemical Cell Microscopy, *Anal. Chem.*, 2021, 93(36), 12337–12345, DOI: [10.1021/ACS.ANALCHEM.1C02099/SUPPL\\_FILE/AC1C02099\\_SI\\_001.PDF](https://doi.org/10.1021/ACS.ANALCHEM.1C02099/SUPPL_FILE/AC1C02099_SI_001.PDF).
- 87 P. A. Kempler, R. H. Coridan and L. Luo, Gas Evolution in Water Electrolysis, *Chem. Rev.*, 2024, 10964, DOI: [10.1021/ACS.CHEMREV.4C00211](https://doi.org/10.1021/ACS.CHEMREV.4C00211).
- 88 A. Raveendran, M. Chandran and R. Dhanusuraman, A comprehensive review on the electrochemical parameters and recent material development of electrochemical water splitting electrocatalysts, *RSC Adv.*, 2023, 13(6), 3843–3876, DOI: [10.1039/D2RA07642J](https://doi.org/10.1039/D2RA07642J).
- 89 Y. Liu, *et al.*, Visualization and Quantification of Electrochemical H<sub>2</sub>Bubble Nucleation at Pt, Au, and MoS<sub>2</sub>Substrates, *ACS Sens.*, 2021, 6(2), 355–363, DOI: [10.1021/ACSENSORS.0C00913/SUPPL\\_FILE/SE0C00913\\_SI\\_001.PDF](https://doi.org/10.1021/ACSENSORS.0C00913/SUPPL_FILE/SE0C00913_SI_001.PDF).
- 90 J. Monteiro and K. McKelvey, Scanning Bubble Electrochemical Microscopy: Mapping of Electrocatalytic Activity with Low-Solubility Reactants, *Anal. Chem.*, 2024, 96(24), 9767–9772, DOI: [10.1021/ACS.ANALCHEM.4C00917](https://doi.org/10.1021/ACS.ANALCHEM.4C00917).
- 91 X. Deng, F. Yang, Y. Li, J. Dang and M. Ouyang, Quantitative study on gas evolution effects under large current density in zero-gap alkaline water electrolyzers, *J. Power Sources*, 2023, 555, 232378, DOI: [10.1016/j.jpowsour.2022.232378](https://doi.org/10.1016/j.jpowsour.2022.232378).
- 92 R. Phillips, A. Edwards, B. Rome, D. R. Jones and C. W. Dunnill, Minimising the ohmic resistance of an alkaline electrolysis cell through effective cell design, *Int. J. Hydrogen Energy*, 2017, 42(38), 23986–23994, DOI: [10.1016/j.ijhydene.2017.07.184](https://doi.org/10.1016/j.ijhydene.2017.07.184).
- 93 K. C. Sandeep, *et al.*, Experimental studies and modeling of advanced alkaline water electrolyser with porous nickel electrodes for hydrogen production, *Int. J. Hydrogen Energy*, 2017, 42(17), 12094–12103, DOI: [10.1016/j.ijhydene.2017.03.154](https://doi.org/10.1016/j.ijhydene.2017.03.154).
- 94 M. Höglinger, S. Kartusch, J. Eder, B. Grabner, M. Macherhammer and A. Trattner, Advanced testing methods for proton exchange membrane electrolysis stacks, *Int. J. Hydrogen Energy*, 2024, 77, 598–611, DOI: [10.1016/j.ijhydene.2024.06.118](https://doi.org/10.1016/j.ijhydene.2024.06.118).
- 95 D. Lee, M. Kim, J. Kim, I. Moon and J. Kim, Advanced CFD simulation of two-phase anion exchange membrane water electrolysis, *Int. J. Hydrogen Energy*, 2024, 88, 322–332, DOI: [10.1016/j.ijhydene.2024.09.180](https://doi.org/10.1016/j.ijhydene.2024.09.180).
- 96 R. Vinodh, T. Palanivel, S. S. Kalanur and B. G. Pollet, Recent advancements in catalyst coated membranes for water electrolysis: a critical review, *Energy Adv.*, 2024, 3(6), 1144–1166, DOI: [10.1039/D4YA00143E](https://doi.org/10.1039/D4YA00143E).
- 97 C. Qiu, Z. Xu, F. Y. Chen and H. Wang, Anode Engineering for Proton Exchange Membrane Water Electrolyzers, *ACS Catal.*, 2024, 14(2), 921–954, DOI: [10.1021/ACSCATAL.3C05162](https://doi.org/10.1021/ACSCATAL.3C05162).
- 98 G. Singer, R. Köll, L. Aichhorn, P. Pertl and A. Trattner, Utilizing hydrogen pressure energy by expansion machines – PEM fuel cells in mobile and other potential applications, *Appl. Energy*, 2023, 343, 121056, DOI: [10.1016/j.apenergy.2023.121056](https://doi.org/10.1016/j.apenergy.2023.121056).
- 99 A. Zahedi, H. A. Z. AL-bonsrulah and M. Tafavogh, Conceptual design and simulation of a stand-alone Wind/PEM fuel Cell/Hydrogen storage energy system for off-grid regions, a case study in Kuhin, Iran, *Sustain. Energy Technol. Assessments*, 2023, 57, 103142, DOI: [10.1016/j.seta.2023.103142](https://doi.org/10.1016/j.seta.2023.103142).
- 100 N. Sezer, S. Bayhan, U. Fesli and A. Sanfilippo, A comprehensive review of the state-of-the-art of proton exchange membrane water electrolysis, *Mater. Sci. Energy Technol.*, 2025, 8, 44–65, DOI: [10.1016/j.mset.2024.07.006](https://doi.org/10.1016/j.mset.2024.07.006).
- 101 S. Liu, Y. Wei, M. Wang and Y. Shen, The future of alkaline water splitting from the perspective of electrocatalysts-



- seizing today's opportunities, *Coord. Chem. Rev.*, 2025, **522**, 216190, DOI: [10.1016/J.CCR.2024.216190](https://doi.org/10.1016/J.CCR.2024.216190).
- 102 S. A. Grigoriev, Electrolyzer – Polymer-Electrolyte Membrane Electrolyzer | Overview, *Reference Module in Chemistry, Molecular Sciences and Chemical Engineering*, 2025, 65–78, DOI: [10.1016/B978-0-323-96022-9.00173-0](https://doi.org/10.1016/B978-0-323-96022-9.00173-0).
- 103 M. Riegraf, R. Costa and K. A. Friedrich, Electrolyzer – Solid Oxide Electrolyzer | Overview, *Reference Module in Chemistry, Molecular Sciences and Chemical Engineering*, 2025, 109–122, DOI: [10.1016/B978-0-323-96022-9.00194-8](https://doi.org/10.1016/B978-0-323-96022-9.00194-8).
- 104 J. Chen, S. Wang, Y. Sun, C. Zhang and H. Lv, Multi-dimensional performance evaluation and energy analysis of proton exchange membrane water electrolyzer, *Appl. Energy*, 2025, **377**, 124457, DOI: [10.1016/J.APENERGY.2024.124457](https://doi.org/10.1016/J.APENERGY.2024.124457).
- 105 B. Hasa, *et al.*, Porous transport layer influence on overpotentials in PEM water electrolysis at low anode catalyst loadings, *Appl. Catal. B Environ. Energy*, 2025, **361**, 124616, DOI: [10.1016/J.APCATB.2024.124616](https://doi.org/10.1016/J.APCATB.2024.124616).
- 106 X. Bi, *et al.*, Simulation study on the effect of temperature on hydrogen production performance of alkaline electrolytic water, *Fuel*, 2025, **380**, 133209, DOI: [10.1016/J.FUEL.2024.133209](https://doi.org/10.1016/J.FUEL.2024.133209).
- 107 S. K. Sampangi and L. Röntzsch, Electrolyzer – Polymer-Electrolyte Membrane Electrolyzer | State of the Art Technique and Systems, *Reference Module in Chemistry, Molecular Sciences and Chemical Engineering*, 2025, 79–94, DOI: [10.1016/B978-0-323-96022-9.00237-1](https://doi.org/10.1016/B978-0-323-96022-9.00237-1).
- 108 S. P. Jiang and Q. Li, Fuel Cells – Alkaline Fuel Cell | Performance and Operational Conditions, *Reference Module in Chemistry, Molecular Sciences and Chemical Engineering*, 2025, 448–459, DOI: [10.1016/B978-0-323-96022-9.00142-0](https://doi.org/10.1016/B978-0-323-96022-9.00142-0).
- 109 L. Wan, *et al.*, Key components and design strategy of the membrane electrode assembly for alkaline water electrolysis, *Energy Environ. Sci.*, 2023, **16**(4), 1384–1430, DOI: [10.1039/D3EE00142C](https://doi.org/10.1039/D3EE00142C).
- 110 W. Xu, D. Zhang, T. Wang, J. Lai and L. Wang, Non-platinum-based electrocatalysts for high performance acidic hydrogen evolution reactions in proton exchange membrane water electrolysis, *Appl. Catal. B Environ. Energy*, 2025, **361**, 124626, DOI: [10.1016/J.APCATB.2024.124626](https://doi.org/10.1016/J.APCATB.2024.124626).
- 111 M. Akbari Kenari, A. Sabour Rouhaghdam and G. Barati Darband, Engineering superhydrophilic Ni-Se-P on Ni-Co nanosheets-nanocones arrays for enhanced hydrogen production assisted by hydrazine oxidation reaction, *J. Colloid Interface Sci.*, 2025, **678**, 828–841, DOI: [10.1016/J.JCIS.2024.09.058](https://doi.org/10.1016/J.JCIS.2024.09.058).
- 112 S. R. Arsad, *et al.*, Recent advancement in water electrolysis for hydrogen production: a comprehensive bibliometric analysis and technology updates, *Int. J. Hydrogen Energy*, 2024, **60**, 780–801, DOI: [10.1016/J.IJHYDENE.2024.02.184](https://doi.org/10.1016/J.IJHYDENE.2024.02.184).
- 113 H. Tüysüz, Alkaline water electrolysis for green hydrogen production, *Acc. Chem. Res.*, 2024, **57**, 558–567, DOI: [10.1021/acs.accounts.3c00709](https://doi.org/10.1021/acs.accounts.3c00709).
- 114 X. Gao, *et al.*, Next-Generation Green Hydrogen: Progress and Perspective from Electricity, Catalyst to Electrolyte in Electrocatalytic Water Splitting, *Nano-Micro Lett.*, 2024, **16**(1), 1–49, DOI: [10.1007/S40820-024-01424-2](https://doi.org/10.1007/S40820-024-01424-2).
- 115 X. W. Lv, W. W. Tian and Z. Y. Yuan, Recent Advances in High-Efficiency Electrocatalytic Water Splitting Systems, *Electrochem. Energy Rev.*, 2023, **6**(1), 1–38, DOI: [10.1007/S41918-022-00159-1](https://doi.org/10.1007/S41918-022-00159-1).
- 116 J. Aicart, *et al.*, Lifespan evaluation of two 30-cell electrolyte-supported stacks for hydrogen production by high temperature electrolysis, *Int. J. Hydrogen Energy*, 2024, **60**, 531–539, DOI: [10.1016/J.IJHYDENE.2024.02.239](https://doi.org/10.1016/J.IJHYDENE.2024.02.239).
- 117 J. Ramsebner, P. Linares, A. Hiesl and R. Haas, Techno-economic evaluation of renewable hydrogen generation strategies for the industrial sector, *Int. J. Hydrogen Energy*, 2024, **60**, 1020–1040, DOI: [10.1016/J.IJHYDENE.2024.02.167](https://doi.org/10.1016/J.IJHYDENE.2024.02.167).
- 118 G. R. Berdiyrov, M. E. Madjet and K. A. Mahmoud, First-principles density functional theory calculations of bilayer membranes heterostructures of Ti3C2T2 (Mxene)/graphene and agnps, *Membranes*, 2021, **11**(7), 543, DOI: [10.3390/membranes11070543](https://doi.org/10.3390/membranes11070543).
- 119 G. S. Cassol, *et al.*, Ultra-fast green hydrogen production from municipal wastewater by an integrated forward osmosis-alkaline water electrolysis system, *Nat. Commun.*, 2024, **15**(1), 1–10, DOI: [10.1038/s41467-024-46964-8](https://doi.org/10.1038/s41467-024-46964-8).
- 120 C. Yan, Y. Zou, Z. Wu and A. Maleki, Effect of various design configurations and operating conditions for optimization of a wind/solar/hydrogen/fuel cell hybrid microgrid system by a bio-inspired algorithm, *Int. J. Hydrogen Energy*, 2024, **60**, 378–391, DOI: [10.1016/J.IJHYDENE.2024.02.004](https://doi.org/10.1016/J.IJHYDENE.2024.02.004).
- 121 B. Amini Horri and H. Ozcan, Green hydrogen production by water electrolysis: current status and challenges, *Curr. Opin. Green Sustain. Chem.*, 2024, **47**, 100932, DOI: [10.1016/J.COGSC.2024.100932](https://doi.org/10.1016/J.COGSC.2024.100932).
- 122 H. K. Thakkar, *et al.*, Photo-sensitive CuS/NiO heterostructure electrocatalysts for energy-saving hydrogen evolution reaction at all pH conditions, *Int. J. Hydrogen Energy*, 2023, **48**(97), 38266–38278, DOI: [10.1016/j.ijhydene.2023.06.014](https://doi.org/10.1016/j.ijhydene.2023.06.014).
- 123 K. K. Joshi, P. M. Pataniya, G. Bhadu and C. K. Sumesh, Monometallic, bimetallic, and trimetallic chalcogenide-based electrodes for electrocatalytic hydrogen evolution reaction, *Int. J. Hydrogen Energy*, 2022, 7260, DOI: [10.1016/j.ijhydene.2022.11.088](https://doi.org/10.1016/j.ijhydene.2022.11.088).
- 124 Z. Cui, *et al.*, Design and Synthesis of Noble Metal-Based Alloy Electrocatalysts and Their Application in Hydrogen Evolution Reaction, *Small*, 2023, **19**(35), 2301465, DOI: [10.1002/SMLL.202301465](https://doi.org/10.1002/SMLL.202301465).
- 125 J. Jayabharathi, B. Karthikeyan, B. Vishnu and S. Sriram, Research on engineered electrocatalysts for efficient water splitting: a comprehensive review, *Phys. Chem. Chem. Phys.*, 2023, **25**(13), 8992–9019, DOI: [10.1039/d2cp05522h](https://doi.org/10.1039/d2cp05522h).
- 126 I. Slobodkin, E. Davydova, M. Sananis, A. Breytus and A. Rothschild, Electrochemical and chemical cycle for high-efficiency decoupled water splitting in a near-neutral



- electrolyte, *Nat. Mater.*, 2024, 23(3), 398–405, DOI: [10.1038/s41563-023-01767-y](https://doi.org/10.1038/s41563-023-01767-y).
- 127 X. Yan, *et al.*, A membrane-free flow electrolyzer operating at high current density using earth-abundant catalysts for water splitting, *Nat. Commun.*, 2021, 12(1), 1–9, DOI: [10.1038/s41467-021-24284-5](https://doi.org/10.1038/s41467-021-24284-5).
- 128 W. Hoisang and K. Sakaushi, Key criteria for next-generation dimensionally stable electrodes towards large-scale green hydrogen production by water electrolysis, *Curr. Opin. Electrochem.*, 2022, 36, 101136, DOI: [10.1016/J.COIELEC.2022.101136](https://doi.org/10.1016/J.COIELEC.2022.101136).
- 129 A. Munir, J. Abdul Nasir, T. ul Haq, J. Iqbal, I. Hussain and A. Qurashi, Benchmarking stable Electrocatalysts for green hydrogen production: a chemist perspective, *Coord. Chem. Rev.*, 2024, 521, 216112, DOI: [10.1016/J.CCR.2024.216112](https://doi.org/10.1016/J.CCR.2024.216112).
- 130 M. A. Habib, *et al.*, Ru/NiMnB spherical cluster pillar for highly proficient green hydrogen electrocatalyst at high current density, *J. Energy Chem.*, 2025, 100, 397–408, DOI: [10.1016/J.JECHEM.2024.08.060](https://doi.org/10.1016/J.JECHEM.2024.08.060).
- 131 R. M. S. Yoo, D. Yesudoss, D. Johnson and A. Djire, A Review on the Application of In-Situ Raman Spectroelectrochemistry to Understand the Mechanisms of Hydrogen Evolution Reaction, *ACS Catal.*, 2023, 13(16), 10570–10601, DOI: [10.1021/ACSCATAL.3C01687/ASSET/IMAGES/LARGE/CS3C01687\\_0019.JPEG](https://doi.org/10.1021/ACSCATAL.3C01687/ASSET/IMAGES/LARGE/CS3C01687_0019.JPEG).
- 132 S. Praveen Kumar, P. C. Sharafudeen and P. Elumalai, High entropy metal oxide@graphene oxide composite as electrocatalyst for green hydrogen generation using anion exchange membrane seawater electrolyzer, *Int. J. Hydrogen Energy*, 2023, 48(97), 38156–38171, DOI: [10.1016/J.IJHYDENE.2023.06.121](https://doi.org/10.1016/J.IJHYDENE.2023.06.121).
- 133 B. Wang, *et al.*, A facile and green strategy for mass production of dispersive FeCo-rich phosphides@N,P-doped carbon electrocatalysts toward efficient and stable rechargeable Zn-air battery and water splitting, *J. Mater. Sci. Technol.*, 2024, 182, 1–11, DOI: [10.1016/J.JMST.2023.08.073](https://doi.org/10.1016/J.JMST.2023.08.073).
- 134 A. Gayathri, V. Ashok, M. Sangamithirai, J. Jayabharathi and V. Thanikachalam, In situ hierarchical self-assembly of NiFeHCF nanoparticles on nickel foam: highly active and ultra-stable bifunctional electrocatalysts for water splitting and their environmental assessment towards green energy, *Green Chem.*, 2024, 26(9), 5326–5338, DOI: [10.1039/D4GC00719K](https://doi.org/10.1039/D4GC00719K).
- 135 P. M. Pataniya and C. K. Sumesh, MoS<sub>2</sub> nanosheets on Cu-foil for rapid electrocatalytic hydrogen evolution reaction, *J. Electroanal. Chem.*, 2022, 912(December 2021), 116270, DOI: [10.1016/j.jelechem.2022.116270](https://doi.org/10.1016/j.jelechem.2022.116270).
- 136 Y. Son, *et al.*, Highly efficient water-splitting electrodes with stable operation at 3 A cm<sup>-2</sup> in alkaline media through molecular linker assembly-induced all-in-one structured NiMo and NiFe electrocatalysts, *Appl. Catal., B*, 2024, 343, 123563, DOI: [10.1016/J.APCATB.2023.123563](https://doi.org/10.1016/J.APCATB.2023.123563).
- 137 F. Tang, T. Liu, W. Jiang and L. Gan, Windowless thin layer electrochemical Raman spectroscopy of Ni-Fe oxide electrocatalysts during oxygen evolution reaction, *J. Electroanal. Chem.*, 2020, 871, 114282, DOI: [10.1016/J.JELECHEMA.2020.114282](https://doi.org/10.1016/J.JELECHEMA.2020.114282).
- 138 J. Chen, *et al.*, Correlative in situ analysis of the role of oxygen on ammonia electrooxidation selectivity on NiOOH surfaces, *J. Catal.*, 2024, 438, 115720, DOI: [10.1016/J.JCAT.2024.115720](https://doi.org/10.1016/J.JCAT.2024.115720).
- 139 H. Ze, *et al.*, In Situ Probing the Structure Change and Interaction of Interfacial Water and Hydroxyl Intermediates on Ni(OH)<sub>2</sub> Surface over Water Splitting, *J. Am. Chem. Soc.*, 2024, 146(18), 12538–12546, DOI: [10.1021/JACS.4C00948/SUPPL\\_FILE/JA4C00948\\_SI\\_001.PDF](https://doi.org/10.1021/JACS.4C00948/SUPPL_FILE/JA4C00948_SI_001.PDF).
- 140 Y. Yan, T. Liu and J. Qi, In-situ characterizations for application in water splitting, *Metal Oxides and Related Solids for Electrocatalytic Water Splitting*, 2022, pp. 351–370, DOI: [10.1016/B978-0-323-85735-2.00006-X](https://doi.org/10.1016/B978-0-323-85735-2.00006-X).
- 141 B. Rotonnelli, M. S. D. Fernandes, F. Bournel, J. J. Gallet and B. Lassalle-Kaiser, In situ/operando X-ray absorption and photoelectron spectroscopies applied to water-splitting electrocatalysis, *Curr. Opin. Electrochem.*, 2023, 40, 101314, DOI: [10.1016/J.COIELEC.2023.101314](https://doi.org/10.1016/J.COIELEC.2023.101314).
- 142 D. Mendoza, S. T. Dong and B. Lassalle-Kaiser, In situ/operando X-ray spectroscopy applied to electrocatalytic CO<sub>2</sub> reduction: status and perspectives, *Curr. Opin. Colloid Interface Sci.*, 2022, 61, 101635, DOI: [10.1016/J.COCIS.2022.101635](https://doi.org/10.1016/J.COCIS.2022.101635).
- 143 J. Sen Zhu, H. Yang, W. Zhang, Y. Mao, S. S. Lyu and J. Chen, An In situ Raman study of intermediate adsorption engineering by high-index facet control during the hydrogen evolution reaction, *Inorg. Chem. Front.*, 2020, 7(9), 1892–1899, DOI: [10.1039/D0QI00124D](https://doi.org/10.1039/D0QI00124D).
- 144 Q. Li, S.-M. Li, Y.-H. Wang and J.-F. Li, New horizon of in-situ Raman spectroelectrochemistry on single-crystal surfaces, *Fundam. Res.*, 2024, DOI: [10.1016/J.FMRE.2024.03.024](https://doi.org/10.1016/J.FMRE.2024.03.024).
- 145 A. Haryanto, K. Jung, C. W. Lee and D. W. Kim, In situ infrared, Raman and X-ray spectroscopy for the mechanistic understanding of hydrogen evolution reaction, *J. Energy Chem.*, 2024, 90, 632–651, DOI: [10.1016/J.JECHEM.2023.10.031](https://doi.org/10.1016/J.JECHEM.2023.10.031).
- 146 W. Zheng, Beginner's Guide to Raman Spectroelectrochemistry for Electrocatalysis Study, *Chemistry*, 2023, 3(2), e202200042, DOI: [10.1002/CMTD.202200042](https://doi.org/10.1002/CMTD.202200042).
- 147 K. Ham, S. Bae and J. Lee, Classification and technical target of water electrolysis for hydrogen production, *J. Energy Chem.*, 2024, 95, 554–576, DOI: [10.1016/J.JECHEM.2024.04.003](https://doi.org/10.1016/J.JECHEM.2024.04.003).
- 148 Y. Wu, *et al.*, Coupling Ir single atom with NiFe LDH/NiMo heterointerface toward efficient and durable water splitting at large current density, *Appl. Catal. B Environ. Energy*, 2025, 360, 124548, DOI: [10.1016/J.APCATB.2024.124548](https://doi.org/10.1016/J.APCATB.2024.124548).
- 149 H. Pourrahmani and J. Van Herle, Manufacturing protocol and post processing of ultra-thin gas diffusion layer using advanced scanning techniques, *Sci. Rep.*, 2024, 14(1), 1–10, DOI: [10.1038/s41598-024-63751-z](https://doi.org/10.1038/s41598-024-63751-z).



- 150 Q. Zhang, *et al.*, Machine Learning-Aided Design of Highly Conductive Anion Exchange Membranes for Fuel Cells and Water Electrolyzers, *Adv. Mater.*, 2024, **36**(36), 2404981, DOI: [10.1002/ADMA.202404981](https://doi.org/10.1002/ADMA.202404981).
- 151 H. Ouabi, R. Lajouad, M. Kissaoui and A. El Magri, Hydrogen production by water electrolysis driven by a photovoltaic source: a review, *e-Prime*, 2024, **8**, 100608, DOI: [10.1016/J.PRIME.2024.100608](https://doi.org/10.1016/J.PRIME.2024.100608).
- 152 L. Zhang, Z. Shi, Y. Lin, F. Chong and Y. Qi, Design Strategies for Large Current Density Hydrogen Evolution Reaction, *Front. Chem.*, 2022, **10**, 866415, DOI: [10.3389/fchem.2022.866415](https://doi.org/10.3389/fchem.2022.866415).
- 153 J. Kwon, S. Choi, C. Park, H. Han and T. Song, Critical challenges and opportunities for the commercialization of alkaline electrolysis: high current density, stability, and safety, *Mater. Chem. Front.*, 2024, **8**(1), 41–81, DOI: [10.1039/D3QM00730H](https://doi.org/10.1039/D3QM00730H).
- 154 L. He, *et al.*, Three-dimensional porous NiCoP foam enabled high-performance overall seawater splitting at high current density, *J. Mater. Chem. A*, 2024, **12**(5), 2680–2684, DOI: [10.1039/D3TA07898A](https://doi.org/10.1039/D3TA07898A).
- 155 A. Pal, S. Kakran, A. Kumar, A. Ben Youssef, U. P. Singh and A. Sidhu, Powering squarely into the future: a strategic analysis of hydrogen energy in QUAD nations, *Int. J. Hydrogen Energy*, 2024, **49**, 16–41, DOI: [10.1016/j.ijhydene.2023.06.169](https://doi.org/10.1016/j.ijhydene.2023.06.169).
- 156 H. F. Araújo, J. A. Gómez and D. M. F. Santos, Proton-Exchange Membrane Electrolysis for Green Hydrogen Production: Fundamentals, Cost Breakdown, and Strategies to Minimize Platinum-Group Metal Content in Hydrogen Evolution Reaction Electrocatalysts, *Catalysts*, 2024, **14**(12), 845, DOI: [10.3390/catal14120845](https://doi.org/10.3390/catal14120845).
- 157 Y. Zhang, *et al.*, Self-supported NiFe-LDH nanosheets on NiMo-based nanorods as high-performance bifunctional electrocatalysts for overall water splitting at industrial-level current densities, *Nano Res.*, 2024, **17**(5), 3769–3776, DOI: [10.1007/S12274-023-6303-9/METRICS](https://doi.org/10.1007/S12274-023-6303-9/METRICS).
- 158 Z. Li, *et al.*, Recent advances in design of hydrogen evolution reaction electrocatalysts at high current density: a review, *Chin. J. Catal.*, 2024, **63**, 33–60, DOI: [10.1016/S1872-2067](https://doi.org/10.1016/S1872-2067).
- 159 L. Yin, *et al.*, Stable Anion Exchange Membrane Bearing Quinuclidinium for High-performance Water Electrolysis, *Angew. Chem., Int. Ed.*, 2024, **63**(19), e202400764, DOI: [10.1002/ANIE.202400764](https://doi.org/10.1002/ANIE.202400764).
- 160 S. W. Sharshir, A. Joseph, M. M. Elsayad, A. A. Taremi, A. W. Kandeal and M. R. Elkadeem, A review of recent advances in alkaline electrolyzer for green hydrogen production: performance improvement and applications, *Int. J. Hydrogen Energy*, 2024, **49**, 458–488, DOI: [10.1016/j.ijhydene.2023.08.107](https://doi.org/10.1016/j.ijhydene.2023.08.107).

